New Structural Aspects of α-Pyrrolidinonate- and α-Pyridonate-Bridged, Homo- and Mixed-Valence, Di- and Tetranuclear *cis*-Diammineplatinum Complexes: Eight New Crystal Structures, Stoichiometric 1:1 Mixture of $Pt(2.25+)_4$ and $Pt(2.5+)_4$, New Quasi-One-Dimensional Halide-Bridged $[Pt(2.5+)_4\text{-}Cl\cdots]_\infty$ System, and Consideration of Solution Properties

Ken Sakai,*,† Yuko Tanaka,† Yuriko Tsuchiya,† Kentaro Hirata,† Taro Tsubomura,† Seiichiro Iijima,‡ and Ashis Bhattacharjee‡,§

Contribution from the Department of Industrial Chemistry, Seikei University, Kichijoji-Kitamachi, Musashino, Tokyo 180-8633, Japan, and National Institute of Bioscience and Human-Technology, 1-1 Higashi, Tsukuba, Ibaraki 305-8566, Japan

Received January 2, 1998

Abstract: Eight new crystalline α-pyrrolidinonate-bridged homo- and mixed-valence *cis*-diammineplatinum dimers and tetramers, HT-$[Pt(2.0+)_2(NH_3)_4(\mu\text{-}C_4H_6NO)_2](ClO_4)_2$ (**2**), HH-$[Pt(2.25+)_2(NH_3)_4(\mu\text{-}C_4H_6NO)_2]_2(ClO_4)_5$ (**4**), HH-$[Pt(2.25+)_2(NH_3)_4(\mu\text{-}C_4H_6NO)_2]_2(PF_6)_3(NO_3)_2$ (**5**), $\{$HH-$[Pt(2.25+)_2(NH_3)_4(\mu\text{-}C_4H_6NO)_2]_2\}\{$HH-$[Pt(2.5+)_2(NH_3)_4(\mu\text{-}C_4H_6NO)_2(NO_3)]_2\}(PF_6)_2(NO_3)_7\cdot 6H_2O$ (**7**), HH-$[Pt(2.5+)_4(NH_3)_8(\mu\text{-}C_4H_6NO)_4(Cl)](ClO_4)_3Cl_2$ (**9**), HH-$[Pt(3.0+)_2(NH_3)_4(\mu\text{-}C_4H_6NO)_2(Cl)_2](NO_3)_2$ (**11**), HH-$[Pt(3.0+)_2(NH_3)_4(\mu\text{-}C_4H_6NO)_2(Cl)(NO_3)](NO_3)_2\cdot H_2O$ (**12**), and HT-$[(H_2O)(H_3N)_2Pt(3.0+)(\mu\text{-}C_4H_6NO)_2Pt(3.0+)(NH_3)(\mu\text{-}OH)]_2(NO_3)_6\cdot 4H_2O$ (**14**), have been isolated and characterized by X-ray diffraction, where HH and HT correspond to the head-to-head and head-to-tail isomers, respectively. The first spontaneous resolution has been observed for the chiral HT-$Pt(2.0+)_2$ molecules (**2**). **7** has turned out to be the first 1:1 "stoichiometric" mixture of blue and tan ($Pt(2.25+)_4$ and $Pt(2.5+)_4$). The structural evidence supporting the axial coordination behaviors of the $Pt(2.5+)_4$ tetramer has been obtained (**7** and **9**). A very unique quasi-one-dimensional halide-bridged system having a chain definition of $[Pt(2.5+)_4\text{−}Cl\cdots]_\infty$ has been characterized (**9**). The HT-$Pt(3.0+)_2$ dimer has been found to release an NH_3 group in aqueous media to form a dimer of dimers linked by μ-OH bridges (**14**). Relationships between the structural parameters and the average Pt oxidation state have been examined in detail to better understand the structure-transformation properties of the platinum-blue family. Remarkable structural differences observed between the pentacyclic α-pyrrolidinonate and the hexacyclic α-pyridonate systems are rationally interpreted in terms of differences in both the N−C−O bite angle and the Pt−N−C angle around the bridging geometry. In addition, spectrophotometric studies reveal that an outer-sphere electron-transfer process between two $Pt(2.25+)_4$ molecules takes place to afford a $Pt(2.0+)_4$ and a $Pt(2.5+)_4$ molecule. General consideration for the solution properties of this family is also described. The synthesis of an α-pyridonate $Pt(2.5+)_4$ complex is also reported.

Introduction

Since Rosenberg discovered the antitumor activity of *cis*-$Pt(NH_3)_2Cl_2$ (*cis*-DDP), the chemistry of *cis*-DDP and its derivatives has received considerable attention because of their potential application as anticancer drugs.[1] The "platinum-pyrimidine blues" obtained from the hydrolysis product of *cis*-DDP (i.e., *cis*-$[Pt(NH_3)_2(OH_2)_2]^{2+}$) and pyrimidine bases have also attracted attention because of their high index of antitumor activity with a lower associated nephrotoxicity than *cis*-DDP.[1d,e] Consequently, a large number of homo- and mixed-valence, di- and tetranuclear platinum complexes have been isolated and

* To whom correspondence should be addressed. E-mail: ksakai@ch.seikei.ac.jp. Fax: +81-422-37-3871.

† Seikei University.

‡ National Institute of Bioscience and Human-Technology (magnetic susceptibility measurements).

§ Present address: Department of Physics, St. Joseph's College, P. O. North Point, Dt. Darjeeling, West Bengal, India 734104.

(1) (a) Rosenberg, B.; Van Camp, L.; Krigas, T. *Nature (London)* **1965**, *205*, 698. (b) Rosenberg, B.; Van Camp, L.; Trosko, J. E.; Mansour, V. H. *Nature (London)* **1969**, *222*, 385. (c) Rosenberg, B.; Van Camp, L. *Cancer Res.* **1970**, *30*, 1799. (d) Davidson, J. P.; Faber, P. J.; Fisher, R. G., Jr.; Mansy, S.; Peresie, H. J.; Rosenberg, B.; Van Camp, L. *Cancer Chemother. Rep.* **1975**, *59*, 287. (e) Rosenberg, B. *Cancer Chemother. Rep.* **1975**, *59*, 589. (f) Sherman, S. E.; Lippard, S. J. *Chem. Rev.* **1987**, *87*, 1153. (g) Sundquist, W. I.; Lippard, S. J. *Coord. Chem. Rev.* **1990**, *100*, 293. (h) Reedijk, J. *Inorg. Chim. Acta* **1992**, *198*−*200*, 873. (i) Takahara, P. M.; Frederick, C. A.; Lippard, S. J. *J. Am. Chem. Soc.* **1996**, *118*, 12309 and references therein.

(2) Faggiani, R.; Lippert, B.; Lock, C. J. L.; Speranzini, R. A. *J. Am. Chem. Soc.* **1981**, *103*, 1111.

(3) (a) Faggiani, R.; Lock, C. J. L.; Pollock, R. J.; Rosenberg, B.; Turner, G. *Inorg. Chem.* **1981**, *20*, 804. (b) Lippert, B.; Schöllhorn, H.; Thewalt, U. *J. Am. Chem. Soc.* **1986**, *108*, 525. (c) Lippert, B.; Schöllhorn, H.; Thewalt, U. *Inorg. Chem.* **1986**, *25*, 407. (d) Schöllhorn, H.; Eisenmann, P.; Thewalt, U.; Lippert, B. *Inorg. Chem.* **1986**, *25*, 3384. (e) Lippert, B.; Neugebauer, D.; Raudaschl, G. *Inorg. Chim. Acta* **1983**, *78*, 161. (f) Micklitz, W.; Riede, J.; Huber, B.; Müller, G.; Lippert, B. *Inorg. Chem.* **1988**, *27*, 1979. (g) Schöllhorn, H.; Thewalt, U.; Lippert, B. *J. Am. Chem. Soc.* **1989**, *111*, 7213. (h) Trötscher, G.; Micklitz, W.; Schöllhorn, H.; Thewalt, U.; Lippert, B. *Inorg. Chem.* **1990**, *29*, 2541.

S0002-7863(98)00019-5 CCC: $15.00
Published on Web 08/11/1998

structurally characterized.[2−12] The basic unit is made up of a dimeric unit doubly bridged with amidate ligands, $[Pt_2(NH_3)_4(\mu\text{-amidato-}N,O)_2]^{n+}$, for which two geometrical isomers (HH and HT) are known (see Figure 1). Strictly, optical isomers must be taken into consideration for the HT isomer. The amidate ligands used in the previous studies are shown in Figure 2. The tetraplatinum chain structures are achieved only with the HH dimers, and the dimer−dimer interaction is generally stabilized by a Pt−Pt bond and/or four hydrogen bonds formed between the oxygen atoms of amidates and the amines (see Figure 1). On the other hand, the HT dimers do not yield a tetramer, for the association is prohibited by the steric bulks of exocyclic amidate rings at both ends of the unit. However, octanuclear platinum complexes (tetramers of dimers) are given when acyclic amidates, such as acetamidate and 2-fluoroacetamidate (see Figure 2), are employed because of the absence of steric hindrances at the N(amidate)−Pt geometry.[11] Therefore, dimerization of the HT dimers may be possible in these systems.

As for the Pt oxidation state of the HH compounds of exocylic amidates, it is convenient to consider that there are only four oxidation states (2.0+, 2.25+, 2.5+, and 3.0+) and that only one nuclearity dominates in each oxidation level *in solution*. In the lowest oxidation level, the dinuclear HH-$[Pt(2.0+)_2(NH_3)_4(\mu\text{-amidato-}N,O)_2]^{2+}$ complex (abbreviated as $Pt(2.0+)_2$) is believed to be the sole chemical species in aqueous media if the HH−HT isomerization does not take place,[5b,d,e,8a,b] since the crystallographically observed hydrogen-bonded tetramer HH-$[Pt(2.0+)_2(NH_3)_4(\mu\text{-amidato-}N,O)_2]_2^{4+}$ (abbreviated as $Pt(2.0+)_4$) is, presumably, unstable due to the lack of an effective Pt−Pt bond between the two units. The second oxidation level 2.25+ corresponds to the so-called tetranuclear *blue*, $[Pt(2.25+)_2(NH_3)_4(\mu\text{-amidato-}N,O)_2]_2^{5+}$ (abbreviated as $Pt(2.25+)_4$) (formally, $Pt(2.25+)_4 = Pt(II)_3Pt(III)$). One unpaired electron derived from the Pt(III) ion is known to be delocalized over the four platinum centers, which was first evidenced by the EPR

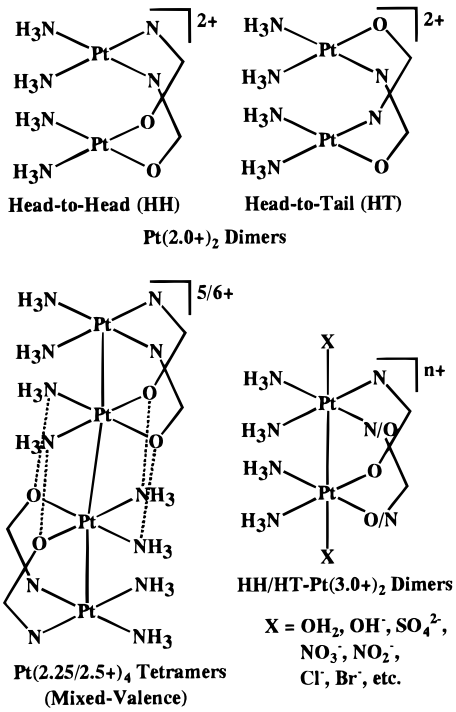

Figure 1. Structures of the platinum-blue complexes, where the term "platinum-blue complex(es)" is introduced as a generic name for this family.

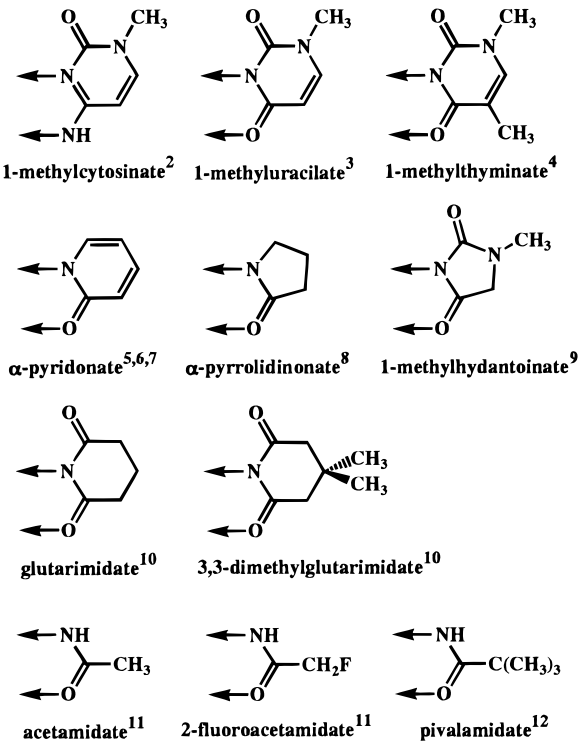

Figure 2. Bridging amidate ligands used for the platinum-blue complexes.

(4) (a) Lippert, B.; Neugebauer, D.; Schubert, U. *Inorg. Chim. Acta* **1980**, *46*, L11. (b) Schöllhorn, H.; Thewalt, U.; Lippert, B. *Inorg. Chim. Acta* **1984**, *93*, 19. (c) Lock, C. J. L.; Peresie, H. J.; Rosenberg, B.; Turner, G. *J. Am. Chem. Soc.* **1978**, *100*, 3371. (d) Micklitz, W.; Renn, O.; Schöllhorn, H.; Thewalt, U.; Lippert, B. *Inorg. Chem.* **1990**, *29*, 1836.

(5) (a) Hollis, L. S.; Lippard, S. J. *J. Am. Chem. Soc.* **1981**, *103*, 1230. (b) Hollis, L. S.; Lippard, S. J. *J. Am. Chem. Soc.* **1983**, *105*, 3494. (c) Hollis, L. S.; Lippard, S. J. *Inorg. Chem.* **1983**, *22*, 2600. (d) O'Halloran, T. V.; Lippard, S. J. *J. Am. Chem. Soc.* **1983**, *105*, 3341. (e) O'Halloran, T. V.; Lippard, S. J. *Inorg. Chem.* **1989**, *28*, 1289.

(6) (a) Barton, J. K.; Rabinowitz, H. N.; Szalda, D. J.; Lippard, S. J. *J. Am. Chem. Soc.* **1977**, *99*, 2827. (b) Barton, J. K.; Best, S. A.; Lippard, S. J.; Walton, R. A. *J. Am. Chem. Soc.* **1978**, *100*, 3785. (c) Barton, J. K.; Szalda, D. J.; Rabinowitz, H. N.; Waszczak, J. V.; Lippard, S. J. *J. Am. Chem. Soc.* **1979**, *101*, 1434. (d) Barton, J. K.; Caravana, C.; Lippard, S. J. *J. Am. Chem. Soc.* **1979**, *101*, 7269. (e) Ginsberg, A. P.; O'Halloran, T. V.; Fanwick, P. E.; Hollis, L. S.; Lippard, S. J. *J. Am. Chem. Soc.* **1984**, *106*, 5430. (f) O'Halloran, T. V.; Roberts, M. M.; Lippard, S. J. *J. Am. Chem. Soc.* **1984**, *106*, 6427. (g) Mascharak, P. K.; Williams, I. D.; Lippard, S. J. *J. Am. Chem. Soc.* **1984**, *106*, 6428. (h) O'Halloran, T. V.; Mascharak, P. K.; Williams, I. D.; Roberts, M. M.; Lippard, S. J. *Inorg. Chem.* **1987**, *26*, 1261.

(7) (a) Hollis, L. S.; Lippard, S. J. *J. Am. Chem. Soc.* **1981**, *103*, 6761. (b) Hollis, L. S.; Lippard, S. J. *Inorg. Chem.* **1983**, *22*, 2605. (c) Hollis, L. S.; Roberts, M. M.; Lippard, S. J. *Inorg. Chem.* **1983**, *22*, 3637. (d) O'Halloran, T. V.; Roberts, M. M.; Lippard, S. J. *Inorg. Chem.* **1986**, *25*, 957.

(8) (a) Matsumoto, K.; Matoba, N. *Inorg. Chim. Acta* **1986**, *120*, L1. (b) Matsumoto, K.; Miyamae, H.; Moriyama, H. *Inorg. Chem.* **1989**, *28*, 2959. (c) Matsumoto, K.; Fuwa, K. *Chem. Lett.* **1984**, 569. (d) Matsumoto, K. *Bull. Chem. Soc. Jpn.* **1985**, *58*, 651. (e) Matsumoto, K.; Takahashi, H.; Fuwa, K. *J. Am. Chem. Soc.* **1984**, *106*, 2049. (f) Matsumoto, K.; Fuwa, K. *J. Am. Chem. Soc.* **1982**, *104*, 897. (g) Matsumoto, K.; Takahashi, H.; Fuwa, K. *Inorg. Chem.* **1983**, *22*, 4086. (h) Abe, T.; Moriyama, H.; Matsumoto, K. *Chem. Lett.* **1989**, 1857. (i) Abe, T.; Moriyama, H.; Matsumoto, K. *Inorg. Chem.* **1991**, *30*, 4198. (j) Matsumoto, K.; Harashima, K. *Inorg. Chem.* **1991**, *30*, 3032. (k) Matsumoto, K.; Watanabe, T. *J. Am. Chem. Soc.* **1986**, *108*, 1308.

(9) Laurent, J.-P.; Lepage, P.; Dahan, F. *J. Am. Chem. Soc.* **1982**, *104*, 7335.

(10) (a) Urata, H.; Moriyama, H.; Matsumoto, K. *Inorg. Chem.* **1991**, *30*, 3914. (b) Matsumoto, K.; Matsunami, J.; Urata, H. *Chem. Lett.* **1993**, 597. (c) Matsumoto, K.; Urata, H. *Chem. Lett.* **1993**, 2061. (d) Matsumoto, K.; Urata, H. *Chem. Lett.* **1994**, 307.

(11) (a) Sakai, K.; Matsumoto, K. *J. Am. Chem. Soc.* **1989**, *111*, 3074. (b) Sakai, K.; Matsumoto, K.; Nishio, K. *Chem. Lett.* **1991**, 1081. (c) Matsumoto, K.; Sakai, K.; Nishio, K.; Tokisue, Y.; Ito, R.; Nishide, T.; Shichi, Y. *J. Am. Chem. Soc.* **1992**, *114*, 8110.

(12) Matsumoto, K.; Matsunami, J.; Mizuno, K.; Uemura, H. *J. Am. Chem. Soc.* **1996**, *118*, 8959.

Table 1. List of Compounds

	chemical formula	bridging amidate	Pt oxdtn state[a]	color	ref	REFC[b]
1	HH-$[Pt_2(NH_3)_4(\mu\text{-}C_4H_6NO)_2]_2(PF_6)_3(NO_3)\cdot H_2O$	α-pyrrolidinonate	$Pt(2.0+)_4$	yellow	8b	JASMOF
2	HT-$[Pt_2(NH_3)_4(\mu\text{-}C_4H_6NO)_2](ClO_4)_2$	α-pyrrolidinonate	$Pt(2.0+)_2$	yellow	this work	
3	HH-$[Pt_2(NH_3)_4(\mu\text{-}C_4H_6NO)_2]_2(PF_6)_2(NO_3)_{2.56}\cdot 5H_2O$	α-pyrrolidinonate	$Pt(2.14+)_4$	violet	8d	CIWNEB
4	HH-$[Pt_2(NH_3)_4(\mu\text{-}C_4H_6NO)_2]_2(ClO_4)_5$	α-pyrrolidinonate	$Pt(2.25+)_4$	blue	this work	
5	HH-$[Pt_2(NH_3)_4(\mu\text{-}C_4H_6NO)_2]_2(PF_6)_3(NO_3)_2$	α-pyrrolidinonate	$Pt(2.25+)_4$	blue	this work	
6	HH-$[Pt_2(NH_3)_4(\mu\text{-}C_4H_6NO)_2]_2(NO_3)_{5.48}\cdot 3H_2O$	α-pyrrolidinonate	$Pt(2.37+)_4$	green	8e	CIMWOK
7	HH-$[Pt_2(NH_3)_4(\mu\text{-}C_4H_6NO)_2]_4(NO_3)_9(PF_6)_2\cdot 6H_2O$	α-pyrrolidinonate	$Pt(2.375+)_4$	green	this work	
8	HH-$[Pt_2(NH_3)_4(\mu\text{-}C_4H_6NO)_2]_2(NO_3)_6\cdot 2H_2O$	α-pyrrolidinonate	$Pt(2.5+)_4$	tan[c]	8f, g	BEKKIL10
9	HH-$[Pt_4(NH_3)_8(\mu\text{-}C_4H_6NO)4(Cl)](ClO_4)_3Cl_2$	α-pyrrolidinonate	$Pt(2.5+)_4$	red	this work	
10	HH-$[Pt_2(NH_3)_4(\mu\text{-}C_4H_6NO)_2(NO_2)(NO_3)](NO_3)_2\cdot H_2O$	α-pyrrolidinonate	$Pt(3.0+)_2$	orange	8h, i	VEWCIJ10
11	HH-$[Pt_2(NH_3)_4(\mu\text{-}C_4H_6NO)_2(Cl)_2](NO_3)_2$	α-pyrrolidinonate	$Pt(3.0+)_2$	yellow	this work	
12	HH-$[Pt_2(NH_3)_4(\mu\text{-}C_4H_6NO)_2(Cl)(NO_3)](NO_3)_2\cdot H_2O$	α-pyrrolidinonate	$Pt(3.0+)_2$	orange	this work	
13	HH-$[(NO_3)(NH_3)_2Pt(\mu\text{-}C_4H_6NO)_2Pt(NH_3)(\mu\text{-}NH_2)]_2(NO_3)_4$	α-pyrrolidinonate	$Pt(3.0+)_4$	yellow	8j	SOLKAF
14	HT-$[(H_2O)(NH_3)_2Pt(\mu\text{-}C_4H_6NO)_2Pt(NH_3)(\mu\text{-}OH)]_2(NO_3)_6\cdot 4H_2O$	α-pyrrolidinonate	$Pt(3.0+)_4$	yellow	this work	
15	HH-$[Pt_2(NH_3)_4(\mu\text{-}C_5H_4NO)_2]_2(NO_3)_4$	α-pyridonate	$Pt(2.0+)_4$	yellow	5a, b	PRDPTA10
16	HH-$[Pt_2(NH_3)_4(\mu\text{-}C_5H_4NO)_2]_2(NO_3)_5\cdot H_2O$	α-pyridonate	$Pt(2.25+)_4$	blue	6a, c	DAMPOP01
17	HH-$[Pt_2(NH_3)_4(\mu\text{-}C_5H_4NO)_2(H_2O)(NO_3)](NO_3)_3\cdot 2H_2O$	α-pyridonate	$Pt(3.0+)_2$	red	7a, b	BAVBAB10
18	HH-$[Pt_2(NH_3)_4(\mu\text{-}C_6H_7N_2O_2)_2](NO_3)_2$	1-methylthyminate	$Pt(2.0+)_2$	yellow	4a, b	MTAPTN10
19	HH-$[Pt_2(NH_3)_4(\mu\text{-}C_5H_5N_2O_2)_2](NO_3)_2\cdot H_2O$	1-methyluracilate	$Pt(2.0+)_2$	yellow	3e	BULWAG
20	HH-$[Pt_2(NH_3)_4(\mu\text{-}C_5H_5N_2O_2)_2]_2(NO_3)_5\cdot 5H_2O$	1-methyluracilate	$Pt(2.25+)_4$	blue	6h	COPPOM10
21	HH-$[Pt_2(NH_3)_4(\mu\text{-}C_4H_5N_2O_2)_2]_2(NO_3)_4\cdot H_2O$	1-methylhydantoinate	$Pt(2.0+)_4$	yellow	9	BOTFIZ

[a] Average platinum oxidation state. [b] Reference codes for the Cambridge Structural Database. [c] Dark red.

study carried out by Lippard's group on an α-pyridonate blue ($S = {}^1/_2$).[6d,e] The third oxidation level 2.5+ corresponds to the tetranuclear $[Pt(2.5+)_2(NH_3)_4(\mu\text{-amidato-}N,O)_2]_2^{6+}$ complex (abbreviated as $Pt(2.5+)_4$) and has been isolated only for the α-pyrrolidinonate family. Therefore, the structural data of the α-pyrrolidinonate $Pt(2.5+)_4$ have been generally adopted in predicting those in other systems.[5b,7b,d] In the highest oxidation level, a Pt−Pt bond formed within the dimeric unit can be regarded as a single bond because of the presence of a filled $\sigma(d_{z^2})$ and a vacant $\sigma^*(d_{z^2})$ orbitals, and the dimer unit prefers to accept two extra donors at both ends of the unit[2,3b−d,7,8h−j] (see Figure 1) rather than to form an interdimer metal−metal bond to give a tetranuclear structure. It was previously proposed that a yellow Pt(III) compound precipitated from an aqueous H_2SO_4 solution is a tetranuclear complex possessing three metal−metal bonds ($[Pt(3.0+)_2(NH_3)_4(\mu\text{-α-pyrrolidinonato-}N,O)_2]_2^{8+}$).[8k] However, recent equilibrium studies[13−15] revealed that the Pt(III) species primarily behave as dimers in solution, and the complex mentioned above is likely to be a sulfato-coordinated dimer, $[Pt(3.0+)_2(NH_3)_4(\mu\text{-α-pyrrolidinonato})_2(SO_4)X]$ (X = OH_2, ClO_4, or SO_4) (abbreviated as $Pt(3.0+)_2$, X−$Pt(3.0+)_2$−X, etc.). Although there is one example of $Pt(3.0+)_4$ which was reported to be a μ-NH_2-bridged dimer of dimers,[8j] no metal−metal bond is formed between the two dimeric units. In addition, there are many examples of structurally analyzed $Pt(3.0+)_2$ dimers of other amidates that possess one or two axial stabilizing donors, such as OH_2,[3d,7a,b] NO_3^-,[3d,7a,b,d,8h,i] NO_2^- (nitro),[2,3b,7c,d,8h,i] Cl^-,[3c,7c] and Br^-.[7c]

Besides interest in their chemotherapeutic activity,[1d,e,16] the platinum-blue complexes possess various intriguing chemical properties. One of the most attractive features lies in the structural flexibility of the basic unit; it is capable of changing the bridged Pt−Pt distance upon changing the average Pt oxidation state.[7d,8e] Another feature is related to the characteristic two-electron one-step redox process based on the $Pt(2.0+)_2$/$Pt(3.0+)_2$ couple.[7a,b,8a] Moreover, the axially exposed d_{z^2} orbitals may be utilized as a coordination site to activate a small molecule: activation of O_2,[14] activation of H_2O to produce O_2,[8k,17] activation of H_2O to produce H_2,[15,18] activation of H_2O_2,[19] epoxidation of olefins via activation of H_2O,[20] and C−H bond activation.[12] Especially, our interest over many years has concentrated on the third one (i.e., catalysis of $Pt(2.0+)_2$ in $H_2O \rightarrow H_2$[15,18]), and our intriguing finding is that *the catalytic activity becomes high as the bridged Pt−Pt distance is shortened*.[21] For example, the α-pyridonate $Pt(2.0+)_2$ (Pt−Pt = 2.8767(7) Å[5a,b]) exhibits higher activity than the α-pyrrolidinonate (Pt−Pt = 3.029(2) Å[8b]).[18] To better understand the structure−activity relationship and to design more efficient catalysts, it has been questioned why such a considerable structural difference should be originated. In this study, the rationale accounting for the difference between the two systems is provided as a result of structural investigations on the eight new crystalline α-pyrrolidinonate compounds (part of this study was presented at the 31st ICCC meeting[22]). The new compounds reported are listed in Table 1, together with 13 relevant compounds selected for comparison in this paper.

On the other hand, solutions of the platinum-blue compounds often involve all four redox species simultaneously. Moreover, ligand substitution equilibria of $Pt(3.0+)_2$ make it more difficult to understand the solution chemistry. However, our recent studies partly unveiled such complicated behaviors.[13−15] One of them revealed that $Pt(2.5+)_4$ rapidly disproportionates and splits into $Pt(2.0+)_2$ and $Pt(3.0+)_2$ after dissolution to aqueous media (eq 1).[13]

(13) Sakai, K.; Tsubomura, T.; Matsumoto, K. *Inorg. Chim. Acta* **1993**, *213*, 11.
(14) Sakai, K.; Tsubomura, T.; Matsumoto, K. *Inorg. Chim. Acta* **1995**, *234*, 157.
(15) Sakai, K. Ph.D. Dissertation, Waseda University, 1993.
(16) Matsunami, J.; Urata, H.; Matsumoto, K. *Inorg. Chem.* **1995**, *34*, 202.
(17) Matsumoto, K.; Matoba, N. *Inorg. Chim. Acta* **1988**, *142*, 59.
(18) (a) Sakai, K.; Matsumoto, K. *J. Coord. Chem.* **1988**, *18*, 169. (b) Sakai, K.; Matsumoto, K. *J. Mol. Catal.* **1990**, *62*, 1. (c) Sakai, K.; Kizaki, Y.; Tsubomura, T.; Matsumoto, K. *J. Mol. Catal.* **1993**, *79*, 141.
(19) Sakai, K.; Matsumoto, K. *J. Mol. Catal.* **1991**, *67*, 7.
(20) Matsumoto, K.; Mizuno, K.; Abe, T.; Kinoshita, J.; Shimura, H. *Chem. Lett.* **1994**, 1325.
(21) (a) Sakai, K.; Takeshita, M.; Goshima, K.; Tsubomura, T. *10th Int. Symp. Photochem. Photophys. Coord. Compd.* **1993**, 109. (b) Sakai, K.; Takeshita, M.; Goshima, K.; Ue, T.; Tsubomura, T. *2nd Int. SPACC Symp.* **1994**, 23 (L7). (c) Shiomi, M.; Sakai, K.; Tsubomura, T. *2nd Int. SPACC Symp.* **1994**, 69 (P10). (d) Sakai, K.; Shiomi, M.; Ikuta, Y.; Tomita, Y.; Kitamura, Y.; Tsubomura, T. *Int. Chem. Congr. Pac. Bas. Soc. (PACIFICHEM)* **1995**, INOR0518.
(22) Sakai, K.; Tanaka, Y.; Tsubomura, T. *31st Int. Conf. Coord. Chem.* **1996**, 85.

$$Pt(2.5+)_4 \rightleftharpoons Pt(2.0+)_2 + Pt(3.0+)_2 \quad (1)$$

The rate of reaction was found to obey $k_{obs} = k_1 + k_2/[H^+]$, and we assumed that this must be due to the presence of an aqua-coordinated and a hydroxo-coordinated $Pt(2.5+)_4$ species, by analogy to the case of $Pt(3.0+)_2$ (eq 2).[3d,14]

$$H_2O-Pt(3.0+)_2-OH_2 \rightleftharpoons H_2O-Pt(3.0+)_2-OH + H^+ \quad (2)$$

Nevertheless, we could not suggest so, due to the lack of strong evidence supporting the axial coordination ability of $Pt(2.5+)_4$, even though the previous structure analysis revealed that two nitrate ions are very weakly associated to the terminal Pt atoms.[8g] In addition, the structural data reported for the "nonstoichiometric mixtures ($Pt(2.14+)_4$ (violet)[8c,d] and $Pt(2.37+)_4$ (green)[8e])" do not provide any solution to this problem. As a result of our tough endeavors in the past years, we also wish to report here on our recent results concerning the solution properties of this family.

Experimental Section

Chemicals. *cis*-$Pt(NH_3)_2Cl_2$ was purchased from N. E. Chemcat. α-Pyrrolidinone (L) (Tokyo Kasei) was purified by distillation before use. All other chemicals (reagent grade) were used as received. Aqueous solutions of *cis*-$[Pt(NH_3)_2(OH_2)_2](NO_3)_2$ (PtN) and *cis*-$[Pt(NH_3)_2(OH_2)_2](ClO_4)_2$ (PtP) were prepared according to the literature method.[23] **8** was prepared as previously described.[13] Spectrophotometric studies were performed using an aqueous H_2SO_4 solution (1.000 M) purchased from Wako (analytical grade).

Syntheses. (a) HT-[Pt(2.0+)$_2$(NH$_3$)$_4$(μ-C$_4$H$_6$NO)$_2$](ClO$_4$)$_2$ (2). To an aqueous solution of PtP (1 mmol/5 mL of H_2O) was added L (1 mmol) followed by adjustment of the pH to 4.1−4.2 with 0.5 M NaOH. The solution was heated at 80 °C for 3 h in air in the dark followed by addition of $NaClO_4$ (4 mmol). Standing of the solution at 5 °C for 2 days afforded slightly bluish (but transparent) plate-needles of **2** (yield, ca. 10%). The crystals of **4** co-deposited were manually removed under a microscope. Anal. Calcd for $Pt_2Cl_2O_{10}N_6C_8H_{24}$: C, 11.64; H, 2.93; N, 10.18. Found: C, 11.62; H, 2.73; N, 9.84.

(b) HH-[Pt(2.25+)$_2$(NH$_3$)$_4$(μ-C$_4$H$_6$NO)$_2$]$_2$(ClO$_4$)$_5$ (4). The synthetic method was almost the same as that of **2** except that a longer reaction time of 4.5 h was applied. Dark blue diamond-shaped crystals of **4** were obtained in 10−20% yield. Anal. Calcd for $Pt_4Cl_5O_{24}N_{12}C_{16}H_{48}$: C, 10.98; H, 2.76; N, 9.60. Found: C, 11.15; H, 2.81; N, 9.79. Quality single crystals of **4** were obtained both by omitting the addition of $NaClO_4$ and by shortening the reaction time. A reaction time of 2−2.5 h and 2−3 weeks of leaving led to the growth of well-formed crystals, even though the yield dropped off.

(c) HH-[Pt(2.25+)$_2$(NH$_3$)$_4$(μ-C$_4$H$_6$NO)$_2$]$_2$(PF$_6$)$_3$(NO$_3$)$_2$ (5). To an aqueous solution of PtN (1 mmol/5 mL of H_2O) was added L (1 mmol) followed by adjustment of the pH to 4.1−4.2 with 0.5 M NaOH. The solution was heated at 80 °C for 2 h in air in the dark followed by addition of KPF_6 (12 mg). Standing of the solution at 5 °C for 1−2 weeks afforded blue plates of **5** (yield, 10−20%). Anal. Calcd for $Pt_4P_3F_{18}O_{10}N_{14}C_{16}H_{48}$: C, 10.61; H, 2.67; N, 10.82. Found: C, 10.86; H, 2.87; N, 11.22.

(d) {HH-[Pt(2.25+)$_2$(NH$_3$)$_4$(μ-C$_4$H$_6$NO)$_2$]$_2$}{HH-[Pt(2.5+)$_2$(NH$_3$)$_4$(μ-C$_4$H$_6$NO)$_2$(NO$_3$)]$_2$}(PF$_6$)$_2$(NO$_3$)$_7$·6H$_2$O (7). To an aqueous solution of PtN (1 mmol/5 mL of H_2O) was added L (1 mmol) followed by adjustment of pH to 4.1−4.2 with 0.5 M NaOH. The solution was heated at 80 °C for 2 h in air in the dark followed by addition of concentrated HNO_3 (0.75 g). $K_2S_2O_8$ (ca. 1 mg) was gradually added to the solution until it became "bluish-green" followed by addition of KPF_6 (12 mg). Standing of the solution at 5 °C for 1 day afforded dark green metallic crystals of **7** in 6% yield, with concomitant deposition of a small amount of red needles (**8**). They were manually separated under a microscope. Anal. Calcd for $Pt_8P_2F_{12}O_{41}N_{33}C_{32}H_{108}$: C, 11.10; H, 3.14; N, 13.35. Found: C, 10.88; H, 3.24; N, 13.27.

(23) Lim, M. C.; Martin, R. B. *J. Inorg. Nucl. Chem.* **1976**, *38*, 1911.

Note: The reproducibility is not so high and probably depends on the overall [Pt(II)]/[Pt(III)] ratio in the synthetic mixture, for this ratio probably controls the $[Pt(2.25+)_4]/[Pt(2.5+)_4]$ ratio according to Scheme 4 (vide infra). Therefore, the optimum condition would be [Pt(II)]/[Pt(III)] = ∼1. Nevertheless, the bluish-green color mentioned above corresponds to $[Pt(2.25+)_4] > [Pt(2.5+)_4]$. This aimed at considering the oxidation process that continues to proceed during the crystal-growing stage.

(e) HH-[Pt(2.5+)$_4$(NH$_3$)$_8$(μ-C$_4$H$_6$NO)$_4$(Cl)](ClO$_4$)$_3$Cl$_2$ (9). **8** (6 μmol, 10 mg) was dissolved in an aqueous 10 mM NaCl solution (0.6 mL). The resulting blue solution was heated at 60−80 °C for a few minutes to completely dissolve **8**. The color of the solution changed to pale green at high temperature, but recooling it to room temperature resulted in recovery of the initial blue color (this is probably because equilibria, such as (1), shift to the side of dimers, leading to loss in both $[Pt(2.25+)_4]$ and $[Pt(2.5+)_4]$). The color of the solution was then adjusted to reddish-brown at room temperature by adding an appropriate amount of $K_2S_2O_8$ (ca. 3 μmol, ca. 0.8 mg). This procedure aimed at minimizing $[Pt(2.25+)_4]$ and maximizing $[Pt(2.5+)_4]$. The temperature of the solution was then raised to 60 °C, and $NaClO_4 \cdot H_2O$ (0.01 g) was dissolved into the solution, followed by filtration of the solution while it was hot in order to remove insoluble materials. Standing of the filtrate at room temperature for 2 h afforded **9** as red, long rectangular thin plates (yield, 10−20%). Anal. Calcd for $Pt_4Cl_6O_{16}N_{12}C_{16}H_{48}$: C, 11.59; H, 2.92; N, 10.14. Found: C, 11.40; H, 2.75; N, 9.91.

(f) HH-[Pt(3.0+)$_2$(NH$_3$)$_4$(μ-C$_4$H$_6$NO)$_2$(Cl)$_2$]Cl$_2$·4H$_2$O (22). **8** (20 mg) was dissolved into a solution of $K_2S_2O_8$ (5 mg) in 0.1 M HCl (2 mL) at 60 °C. Gradual cooling of the solution at room temperature afforded the product as yellow needles (yield, >90%). Anal. Calcd for $Pt_2Cl_4O_6N_6C_8H_{32}$: C, 11.43; H, 3.84; N, 10.00. Found: C, 11.24; H, 3.41; N, 9.78.

(g) HH-[Pt(3.0+)$_2$(NH$_3$)$_4$(μ-C$_4$H$_6$NO)$_2$(Cl)$_2$](NO$_3$)$_2$ (11). **8** (20 mg) was dissolved into a solution of $K_2S_2O_8$ (5 mg) in 0.1 M HCl (0.5 mL), resulting in deposition of yellow needles (**22**). The crystals were completely dissolved at 60 °C by adding concentrated HNO_3 (0.2 mL) and a minimum amount of water followed by filtration of the solution while it was hot. Standing of the filtrate at 5 °C for a few days afforded the product as yellow plates (yield, 50%). Anal. Calcd for $Pt_2Cl_2O_8N_8C_8H_{24}$: C, 11.70; H, 2.95; N, 13.64. Found: C, 12.16; H, 3.09; N, 13.28.

(h) HH-[Pt(3.0+)$_2$(NH$_3$)$_4$(μ-C$_4$H$_6$NO)$_2$(Cl)(NO$_3$)](NO$_3$)$_2$·H$_2$O (12). **8** (20 mg) was dissolved into a solution of $K_2S_2O_8$ (5 mg) in 0.05 M HCl (0.5 mL). The yellow needles deposited were redissolved in a similar manner as for **11**. Gradual concentration of the filtrate at 5 °C in air over several days yielded the product as orange prisms (yield, 30%). Anal. Calcd for $Pt_2ClO_{12}N_9C_8H_{26}$: C, 11.10; H, 3.03; N, 14.56. Found: C, 11.00; H, 3.05; N, 14.46.

(i) HT-[(H$_2$O)(H$_3$N)$_2$Pt(3.0+)(μ-C$_4$H$_6$NO)$_2$Pt(3.0+)(NH$_3$)(μ-OH)]$_2$(NO$_3$)$_6$·4H$_2$O (14). **8** (10 mg) was dissolved in an aqueous 50 mM H_2SO_4 solution (0.5 mL). The solution was heated at 60 °C for 30 min followed by addition of $K_2S_2O_8$ (2.5 mg) and $NaNO_3$ (0.05 g). Standing of the solution at 5 °C for several days afforded an extremely small quantity of the product as yellow prisms (yield, <1%). Since both the yield and the reproducibility were extremely low, elemental analysis could not be carried out. Nevertheless, the structure analysis of the product is so successful that we have no doubt of its chemical formula.

For all the α-pyrrolidinonate compounds described above, cocrystallization of acid is not likely to be promoted, since the complex charges resulting from the proposed formula do not contradict the Pt oxidation levels indicated by the X-ray studies (vide infra).

(j) HH-[Pt(2.5+)$_2$(NH$_3$)$_4$(μ-C$_5$H$_4$NO)$_2$]$_2$(NO$_3$)$_6$·2H$_2$O (α-Pyridonate Tan). A synthetic solution containing PtN (1 mmol) and α-pyridone (1 mmol) was prepared, and the pH was adjusted to 7, according to the method of Barton.[6b] The solution was evaporated to half of the original volume, resulting in deposition of a white solid. This suspension was heated at 80 °C for 30−60 min and was further incubated at 38.5 °C for 24 h followed by filtration to remove insoluble materials. About 1 mL of concentrated HNO_3 was added to the filtrate to adjust the pH to 1 followed by addition of $NaNO_3$ (0.75 g), during

Table 2. Crystallographic Data for **2**, **4**, **5**, **7**, **9**, **11**, **12**, and **14**

	2	**4**	**5**	**7**
formula	$Pt_2Cl_2O_{10}N_6C_8H_{24}$	$Pt_4Cl_5O_{24}N_{12}C_{16}H_{48}$	$Pt_4P_3F_{18}O_{10}N_{14}C_{16}H_{48}$	$Pt_8P_2F_{12}O_{41}N_{33}C_{32}H_{108}$
fw	825.40	1750.25	1811.90	3462.06
cryst color, habit	colorless, plate	dark blue, prism	dark blue, plate	metallic green, prism
cryst size, mm	0.25 × 0.08 × 0.03	0.30 × 0.30 × 0.20	0.23 × 0.23 × 0.01	0.35 × 0.18 × 0.07
cryst syst	monoclinic	monoclinic	monoclinic	triclinic
space group	$P2_1$	$C2/c$	$C2/c$	$P\bar{1}$
a, Å	10.374(2)	17.908(5)	18.277(7)	15.051(2)
b, Å	7.784(5)	9.755(5)	9.801(9)	17.201(2)
c, Å	13.100(4)	25.754(4)	26.03(1)	9.8802(6)
α, deg				96.939(8)
β, deg	103.47(2)	96.69(2)	95.18(4)	92.703(8)
γ, deg				64.404(9)
V, Å^3; Z	1028.7(8); 2	4468(3); 4	4644(5); 4	2290.0(5); 1
ρ_{calcd}, g/cm^3	2.6646	2.6017	2.5916	2.5105
μ, cm^{-1} (radiation)	280.13 (Cu Kα)	128.74 (Mo Kα)	242.16 (Cu Kα)	236.71 (Cu Kα)
trans coeff	0.6235−1.0000[a]	0.7296−1.0000[b]	0.8979−1.0000[a]	0.8985−1.0000[a]
2θ range, deg	6.9−120	5.0−55	3.4−120	5.7−100
total decay, %	none	0.64[c]	0.79	none
no. of total reflns	1763	7090	3845	4947
no. of unique reflns	1690	6885	3698	4710
no. of reflns used[d]	1569	3568	2428	4294
no. of params refined	251	248	180	485
R,[e] R_w[f]	0.0400, 0.0355	0.0565, 0.0426	0.0914, 0.0901	0.0500, 0.0576
weighting scheme, w^{-1}	$\sigma^2(F_o) + 0.0001\|F_o\|^2$	$\sigma^2(F_o) + 0.0001\|F_o\|^2$	$\sigma^2(F_o) + 0.0004\|F_o\|^2$	$\sigma^2(F_o) + 0.0004\|F_o\|^2$

	9	**11**	**12**	**14**
formula	$Pt_4Cl_6O_{16}N_{12}C_{16}H_{48}$	$Pt_2Cl_2O_8N_8C_8H_{24}$	$Pt_2ClO_{12}N_9C_8H_{26}$	$Pt_4O_{30}N_{16}C_{16}H_{56}$
fw	1657.70	821.41	865.98	1733.07
cryst color, habit	red, plate-needle	yellow, plate	orange, prism	yellow, plate
cryst size, mm	0.60 × 0.20 × 0.03	0.30 × 0.30 × 0.10	0.30 × 0.20 × 0.20	0.30 × 0.30 × 0.10
cryst syst	monoclinic	triclinic	monoclinic	triclinic
space group	$P2_1/n$	$P\bar{1}$	$P2_1/a$	$P\bar{1}$
a, Å	9.999(5)	10.114(2)	9.521(3)	10.492(3)
b, Å	26.98(1)	11.988(3)	24.608(7)	11.864(3)
c, Å	17.427(4)	8.789(2)	10.137(2)	9.856(2)
α, deg		100.82(2)		106.41(2)
β, deg	95.23(3)	95.96(1)	110.87(2)	92.20(2)
γ, deg		79.61(1)		100.92(2)
V, Å^3; Z	4682(3); 4	1026.8(4); 2	2219(1); 4	1150.1(5); 1
ρ_{calcd}, g/cm^3	2.3518	2.6567	2.5919	2.5023
μ, cm^{-1} (radiation)	123.23 (Mo Kα)	139.22 (Mo Kα)	127.89 (Mo Kα)	122.35 (Mo Kα)
trans coeff	0.9031−1.0000[a,g]	0.1578−1.0000[b]	0.5784−1.0000[b]	0.5384−1.0000[b]
2θ range, deg	3.0−50	3.5−60	4.5−55	5.0−60
total decay, %	6.21[c]	4.23[c]	1.12[c]	0.74[c]
no. of total reflns	7358	5004	5538	7034
no. of unique reflns	7339	4732	5237	6704
no. of reflns used[d]	3045	3660	3661	5002
no. of params refined	253	253	259	296
R,[e] R_w[f]	0.1019, 0.0950	0.0492, 0.0570	0.0525, 0.0411	0.0445, 0.0314
weighting scheme, w^{-1}	$\sigma^2(F_o) + 0.0004\|F_o\|^2$	$\sigma^2(F_o) + 0.0004\|F_o\|^2$	$\sigma^2(F_o) + 0.0001\|F_o\|^2$	$\sigma^2(F_o)$

[a] DIFABS. [b] North's method. [c] A linear decay correction was applied. [d] With $I > 2.0\sigma(I)$. [e] $R = \sum||F_o| - |F_c||/\sum|F_o|$. [f] $R_w = [\sum|w(|F_o| - |F_c|)^2/\sum|w|F_o|^2]^{1/2}$. [g] Ψ-scan data could not be measured due to the crystal decomposition.

which time the color of the solution became deep blue. Standing of the solution at 5 °C for 24 h afforded the product as dark red needles (yield, 7%). Anal. Calcd for $Pt_4O_{24}N_{18}C_{20}H_{44}$: C, 14.12; H, 2.61; N, 14.82. Found: C, 14.54; H, 2.38; N, 14.41. It should be noted that this sample was free of the blue crystals reported by Barton.

X-ray Crystallography. Crystals obtained above were used without further treatment. Each crystal was mounted on a glass fiber. Diffraction data at 23 °C were measured on a Rigaku AFC-5S diffractometer. For the very small crystals (**2**, **5**, and **7**), graphite-monochromated Cu Kα (1.541 78 Å) radiation was used to improve the reflection/parameter ratios, regardless of their high μ values (Table 2). Graphite monochromated Mo Kα (0.710 69 Å) radiation was used for the remainder of the samples. All the data sets, except for **4** (ω), were collected with the $\omega-2\theta$ scan technique (16 deg/min for **9** and 8 deg/min for the rest). All data sets were corrected for Lorentz and polarization effects and for absorption either by employing Ψ scans on several reflections with χ near 90°[24] or by using the DIFABS program[25] (Table 2). A linear decay correction was also applied to the data, if necessary (Table 2). Metal atom positions were determined by direct methods (SAPI91[26] for **5** and SIR88[27] for the rest), and the remaining non-hydrogen atoms were located using both the DIRDIF[28] program and the difference Fourier techniques. Typically, all non-hydrogen atoms were refined anisotropically by full-matrix least squares. All hydrogen atoms, excluding those of water molecules and a hydroxide ion in **14**, were located in their idealized positions (C−H =

(24) North, A. C. T.; Phillips, D. C.; Mathews, F. S. *Acta Crystallogr.* **1968**, *A24*, 351.
(25) DIFABS: Walker, N.; Stuart, D. *Acta Crystallogr.* **1983**, *A39*, 158.
(26) SAPI91: Fan, H.-F. *Structure Analysis Programs with Intelligent Control*; Rigaku Corporation: Tokyo, Japan, 1991.
(27) SIR88: Burla, M. C.; Camalli, M.; Cascarano, G.; Giacovazzo, C.; Polidori, G.; Spagna, R.; Viterbo, D. *J. Appl. Crystallogr.* **1989**, *22*, 389.
(28) DIRDIF: Parthasarathi, V.; Beurskens, P. T.; Slot, H. J. B. *Acta Crystallogr.* **1983**, *A39*, 860.

0.95 and N−H = 0.87 Å), were included in the final refinements, and were not refined. All the calculations were performed using the teXsan[29] software. Crystallographic data are summarized in Table 2. Positional and thermal parameters and bond lengths and angles are supplied as Supporting Information. Other details on each crystallography data set are described below.

(a) Structure Analysis of HT-[Pt(2.0+)$_2$(NH$_3$)$_4$(μ-C$_4$H$_6$NO)$_2$](ClO$_4$)$_2$ (2). The absolute configuration of this chiral HT-Pt(2.0+)$_2$ was determined by comparing the final reliability factors refined for two possibilities.

(b) Structure Analysis of HH-[Pt(2.25+)$_2$(NH$_3$)$_4$(μ-C$_4$H$_6$NO)$_2$]$_2$(ClO$_4$)$_5$ (4). One of the perchlorate ions had to be refined under the rigid group constraint (Cl−O = 1.43 Å), where the central Cl ion was refined anisotropically and the isotropic temperature factors of four oxygen atoms were constrained to be equal.

(c) Structure Analysis of HH-[Pt(2.25+)$_2$(NH$_3$)$_4$(μ-C$_4$H$_6$NO)$_2$]$_2$(PF$_6$)$_3$(NO$_3$)$_2$ (5). As a result of the low quality of the reflection data, all the carbon atoms were treated isotropically. Of one and a half PF_6^- ions and one NO_3^- ion in the asymmetric unit, only a half of PF_6^- locating on a 2-fold axis was treated anisotropically. The remainder were located under the rigid group constraint (P−F = 1.53 and N−O = 1.22 Å), even though most of them were clearly visible. The isotropic temperature factors of them were individually refined.

(d) Structure Analysis of {HH-[Pt(2.25+)$_2$(NH$_3$)$_4$(μ-C$_4$H$_6$NO)$_2$]$_2$}{HH-[Pt(2.5+)$_2$(NH$_3$)$_4$(μ-C$_4$H$_6$NO)$_2$(NO$_3$)]$_2$}(PF$_6$)$_2$(NO$_3$)$_7$·6H$_2$O (7). All the non-hydrogen atoms within the complex cations were treated anisotropically. Water molecules were treated isotropically. Counterions were partially disordered over two sites, and most of them were visible. This might suggest that part of the counterions are packed in the space group $P1$. Nevertheless, we finally decided to solve this structure by selecting $P\bar{1}$, for the main cationic moieties were well treated with normal temperature factors. Of one PF_6^- ion involved in the asymmetric unit, a half locating at an inversion center was treated anisotropically, while the other half was located at a general position and was refined under the rigid group constraint (P−F = 1.53 Å, occupancy factor = 0.5). Of four and a half NO_3^- ions in the asymmetric unit, two were located on a general position and refined anisotropically. The other 2.5 were found to be disordered over five sites and were treated under the rigid group constraint (N−O = 1.22 Å, occupancy factor = 0.5), where the isotropic temperature factors within each group were constrained to be equal.

(e) Structure Analysis of HH-[Pt(2.5+)$_4$(NH$_3$)$_8$(μ-C$_4$H$_6$NO)$_4$(Cl)](ClO$_4$)$_3$Cl$_2$ (9). The reflection data with $2\theta > 50°$ could not be appropriately measured because of the seriously damaged nature of the crystal. As a result, the data with $2\theta < 50°$ were used in the calculations. Only four Pt and one Cl atoms within the complex cation were refined anisotropically, and the remaining non-hydrogen atoms were treated isotropically. Two noncoordinated Cl^- ions were both found to be disordered over two sites (A and B sites). For each case, the occupancy factors were refined under the constraint defined with occupancy(A) + occupancy(B) = 1 (0.67(3) for Cl(5A), 0.33(3) for Cl(5B), 0.44(3) for Cl(6A), 0.56(3) for Cl(6B)).

(f) Structure Analysis of HH-[Pt(3.0+)$_2$(NH$_3$)$_4$(μ-C$_4$H$_6$NO)$_2$(Cl)$_2$](NO$_3$)$_2$ (11). All non-hydrogen atoms were refined anisotropically. Relatively large residual peaks ($\Delta(\rho)_{max}$ = 5.46 e/A^3) observed in the final difference Fourier map were all located near the Pt atoms.

(g) Structure Analysis of HH-[Pt(3.0+)$_2$(NH$_3$)$_4$(μ-C$_4$H$_6$NO)$_2$(Cl)(NO$_3$)](NO$_3$)$_2$·H$_2$O (12). The axially coordinated nitrate ion was found to be disordered over two sites, which were both treated isotropically. Occupancy factors of them were first independently refined, found to have an equal population, and finally fixed at 0.5. Since the central nitrogen atoms of these disordered nitrates were observed to be overlapped, they were regarded as a single atom. On the other hand, one of the two counterions was also treated as being disordered over two sites and was refined under the rigid group constraint (N−O = 1.22 Å, occupancy factor = 0.5 for each site), where the isotropic temperature factors within each rigid group were constrained to be equal. A water molecule was similarly treated to be disordered over two sites (occupancy factor = 0.5). All the remaining non-hydrogen atoms were refined anisotropically.

Chart 1

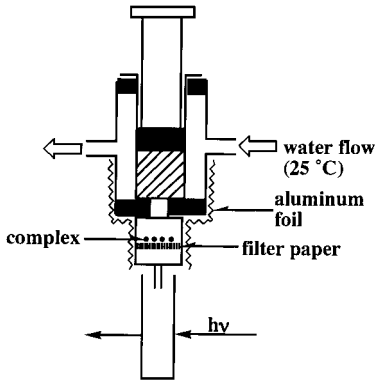

(h) Structure Analysis of HT-[(H$_2$O)(H$_3$N)$_2$Pt(3.0+)(μ-C$_4$H$_6$NO)$_2$Pt(3.0+)(NH$_3$)(μ-OH)]$_2$(NO$_3$)$_6$·4H$_2$O (14). All non-hydrogen atoms were treated aniosotropically. One of the three counterions was treated as being disordered over two sites, in which occupancy factors of two sites A and B were refined under the constraint defined with occupancy(A) + occupancy(B) = 1.0 (occupancy(A) = 0.34(1) and occupancy(B) = 0.66(1)). The bridging atom connecting the two dimeric units was at first assumed to be a nitrogen atom of μ-NH$_2$. However, the anisotropic thermal parameters fell into negative values, and satisfactory convergence was rather achieved when the atom was treated as an oxygen atom. We finally judged that the atom must be derived from μ-OH.

Magnetic Susceptibility Measurements. After the sample was placed inside the measuring chamber, the whole chamber was thoroughly evacuated (for ca. 2 days) at 10^{-6} Torr and then flushed with dry He gas several times by repeated evacuation to avoid the effect of oxygen. Finally, a small amount of dry He gas was introduced inside the chamber. The molar magnetic susceptibility was measured under an applied magnetic field of 4.65 kG on a Faraday balance, consisting of a Cahn 2000 microbalance. The conventional HgCo(SCN)$_4$ standard was used to calibrate the instrument, and the necessary diamagnetic corrections were made.

UV−Visible Spectroscopy. Spectra in Figure 10 were recorded on a Shimadzu UV-2100S spectrophotometer. Dead time spent for the complete dissolution of **4** was 18 s, and time consumed in scanning each spectrum was 33 s. Additionally, we have repeatedly ascertained that the formation of Pt(2.5+)$_4$ (band at 478 nm) after dissolution of Pt(2.25+)$_4$ (**4**) is unobservably rapid even if the dead time is diminished to ca. 1 s. To perform quick dissolution, a solid sample was placed inside a syringe filter and then a solution stored in a syringe whose temperature was thermostatically controlled at 25 °C was quickly flushed though the filter to transfer a freshly prepared solution into the measurement cell (see Chart 1). After the injection, spectral changes (400−800 nm) were monitored every 60 ms on a Hamamatsu PMA-11 diode-array detector using a tungsten lamp as a light source. However, the same decay processes as Figure 10 were observed (data not shown). The similar experiments were further performed several times by dissolving either **4** or **8**, using UV-2100S. In all the experiments, the concentration of the complex dissolved was calibrated from the final absorbance at 286 and 362 nm. The molar absorptivities of Pt(3.0+)$_2$ at these wavelengths were separately determined as 1.63(1) × 10^4 and 2.49(1) × 10^3 M^{-1} cm^{-1} (1 M H$_2$SO$_4$, 25 °C), respectively (*both bands obey Beer's law*). In the determination, five solutions of **8** were prepared at different concentrations (4.21 × 10^{-5} to 2.19 × 10^{-4} M). Each solution was incubated at 50 °C until the red chromophore of Pt(2.5+)$_4$ disappeared, and then all the chemical species in solution were completely oxidized into Pt(3.0+)$_2$ by adding a minimum amount of $K_2S_2O_8$ (0.13−0.15 mg/3 mL) (*Note*: $K_2S_2O_8$ neither effectively absorbs light above 250 nm (ϵ < 20) nor affects the spectrum of Pt(3.0+)$_2$). Each solution was further incubated at 50 °C until growth of the bands ceased, and absorbance less than 2 was measured at each maximum wavelength using three cells of different

(29) teXsan: *Single Crystal Structure Analysis Software*, version 1.6f; Molecular Structure Corporation: The Woodlands, TX, 1994.

Table 3. Comparison of the Structural Features

	amidate ligand	*a*	Pt−Pt, intra[b] (Å)	Pt−Pt, inter[c] (Å)	Pt−Pt−Pt (deg)	τ[d] (deg)	ω[e] (deg)	O−C−N (deg)	Pt−N−C (deg)	Pt−O−C (deg)	O···N[f] (Å)
1	α-pyrrolidinonate	2.0+	3.029(2)	3.185(2)	157.94(5)	35.9	1.0	126(3)	125(2)	130(2)	2.30[i]
								127(2)	129(1)	127(2)	2.28[i]
2	α-pyrrolidinonate	2.0+	3.085(1)	5.8515(7)	*g*	37.6	2.3	127(2)	129(1)	125(1)	2.31(3)
								126(2)	128(1)	128(1)	2.29(3)
3	α-pyrrolidinonate	2.14+ (**3a**)	2.848(2)	2.875(2)	166.53(6)	26.2	0.5[i]	129(3)	123(2)	122(2)	2.33[i]
							2.0[h,i]	127(3)	126(2)	123(2)	2.33[i]
		2.14+ (**3b**)	2.839(2)	2.875(2)	168.31(6)	23.5[i]	6.3[i]	124(3)	120(3)	122(2)	2.28[i]
							0[h,i]	121(3)	132(2)	122(2)	2.58[i]
4	α-pyrrolidinonate	2.25+	2.8780(9)	2.894(1)	165.57(4)	29.2	6.1	128(1)	126(1)	121(1)	2.29(1)
							1.2[h]	125(1)	129(1)	122(1)	2.30(1)
5	α-pyrrolidinonate	2.25+	2.840(2)	2.868(3)	167.3(1)	28.0	4.3	125(4)	124(2)	125(2)	2.24(4)
							1.5[h]	128(3)	129(2)	119(2)	2.30(4)
6	α-pyrrolidinonate	2.37+ (**6a**)	2.764(8)	2.739(8)	166.6(3)	24.5	3.8[i]	110(8)	132(5)	133(7)	2.18[i]
			2.740(8)		167.2(3)	17.4[i]	6.3[i]	117(8)	132(7)	120(7)	2.29[i]
						3.56[h,i]	30.5[h,i]	116(8)	128(8)	128(7)	2.24[i]
								113(9)	114(7)	114(6)	2.35[i]
		2.37+ (**6b**)	2.761(8)	2.724(8)	168.5(3)	26.9	2.3[i]	119(8)	127(7)	127(8)	2.16[i]
			2.753(9)		170.9(3)	17.1[i]	5.0[i]	120(9)	124(8)	128(8)	2.20[i]
						10.0[h,i]	33.3[h,i]	134(9)	116(8)	119(8)	2.40[i]
								133(11)	112(7)	110(5)	2.43[i]
7	α-pyrrolidinonate	2.25+ (**7a**)	2.862(1)	2.864(2)	166.50(4)	28.1	1.7	121(2)	130(2)	125(1)	2.24(3)
							0[h]	125(2)	128(1)	123(1)	2.25(3)
		2.5+ (**7b**)	2.719(1)	2.818(2)	169.78(5)	21.4	2.1	123(1)	128(1)	119(1)	2.29(2)
							1[h]	124(1)	125(1)	121(1)	2.31(2)
8	α-pyrrolidinonate	2.5+	2.702(6)	2.710(5)	170.4(1)	17.9[i]	1.3[i]	127(6)	120(6)	119(6)	2.32[i]
			2.706(6)		168.8(1)	20.6[i]	1.3[i]	121(3)	120(4)	104(3)	2.28[i]
						1.6[h,i]	29.5[h,i]	118(6)	129(8)	121(5)	2.46[i]
								147(5)	109(5)	111(3)	2.49[i]
9	α-pyrrolidinonate	2.5+	2.701(4)	2.724(4)	171.6(1)	21.8	3.0	132(9)	124(6)	127(4)	2.24(7)
			2.793(4)		168.3(1)	24.2	4.0	113(6)	130(4)	115(5)	2.25(8)
						3.6[h]	35.8[h]	130(10)	126(7)	116(5)	2.30(8)
								141(7)	117(4)	116(4)	2.24(7)
10	α-pyrrolidinonate	3.0+	2.644(1)	*g*	*g*	19.6	0.0	125(1)	125(1)	120(1)	2.30[i]
								128(1)	123(1)	118(1)	2.33[i]
11	α-pyrrolidinonate	3.0+	2.6366(7)	*g*	*g*	18.9	1.5	125(1)	124(1)	120(1)	2.28(2)
								125(1)	124(1)	120(1)	2.29(1)
12	α-pyrrolidinonate	3.0+	2.6239(9)	*g*	*g*	19.6	0.7	124(1)	125(1)	120(1)	2.28(2)
								123(1)	125(1)	121(1)	2.29(2)
13	α-pyrrolidinonate	3.0+	2.608(1)	3.160[i]	*g*	17.7	0.4	124[i]	122[i]	121[i]	2.33[i]
								124[i]	126[i]	118[i]	2.31[i]
14	α-pyrrolidinonate	3.0+	2.5527(7)	3.1578(6)	*g*	16.9	10.7	125.3(8)	123.6(6)	117.6(5)	2.28(1)
								124.8(8)	124.6(6)	117.6(5)	2.27(1)
15	α-pyridonate	2.0+	2.8767(7)	3.1294(9)	158.40(3)	30.0	20.3	124(1)	121(1)	125(1)	2.33(1)
								122(1)	124(1)	126(1)	2.30(1)
16	α-pyridonate	2.25+	2.7745(4)	2.8770(5)	164.60(2)	27.4	22.8	121(1)	123(1)	123(1)	2.30(1)
								121(1)	123(1)	123(1)	2.30(1)
17	α-pyridonate	3.0+	2.5401(5)	*g*	*g*	20.0	23.2	120.0(7)	118.9(6)	120.2(5)	2.30(1)
								121.4(8)	121.2(6)	118.4(5)	2.30(1)
18	1-methylthyminate	2.0+	2.927(1)	5.66	*g*	31.4	1.9	120.5(9)	126.2(7)	131.6(6)	2.28[i]
								122.2(9)	125.4(7)	129.9(6)	2.29[i]
19	1-methyluracilate	2.0+	2.937(1)	4.798(1)	*g*	34.1	25.2	122[i]	125[i]	125[i]	2.28[i]
								122[i]	121[i]	126[i]	2.33[i]
20	1-methyluracilate	2.25+	2.810(2)	2.866(2)	165.02(5)	27.3	6.1	117[i]	123[i]	131[i]	2.26[i]
			2.793(2)		164.81(5)	26.4	8.4	126[i]	128[i]	125[i]	2.30[i]
						0.05[h]	22.1[h]	119[i]	125[i]	129[i]	2.29[i]
								125[i]	122[i]	127[i]	2.29[i]
21	1-methylhydantoinate	2.0+	3.131	3.204	160.5	38.6	7.5[i]	131[i]	131[i]	121[i]	2.32[i]
								128[i]	130[i]	124[i]	2.34[i]

[a] Average Pt oxidation state. [b] Bridged Pt−Pt distances. [c] Interdimer Pt−Pt distances. [d] Dihedral cant between the two adjacent platinum coordination planes. [e] Twist angle of the two platinum coordination planes about the Pt−Pt vector. [f] Bite distances of amidates. [g] No interdimer Pt−Pt interaction is achieved. [h] Twist angle for the interdimer association, while the nonlabeled values correspond to the bridged Pt−Pt associations. [i] Calculated by us, where esd's were not estimated.

path lengths (1, 5, and 10 mm). The molar absorptivity of Pt(2.5+)$_4$ at 478 nm was determined as 3.4×10^4 M^{-1} cm^{-1} (1 M H_2SO_4, 25 °C). In the determination, the first-order decay of Pt(2.5+)$_4$ (eq 1) after dissolution of **8** was measured and the initial absorbance given from a least-squares fit was adopted.

Results and Discussion

Important structural parameters determined for the eight new compounds are summarized in Table 3, together with those for the related compounds. We will not discuss the detailed structural features that are fundamentally similar to those reported so far; we would rather concentrate on our new findings in this paper.

Blues. As a result of the lack of structural data for the α-pyrrolidinonate Pt(2.25+)$_4$, it has been inevitably assumed that the Pt−Pt distances of this complex are not much different from those of the α-pyridonate analogue.[8c−g] In this context, we first attempted to determine the crystal structure of this complex. As a result, we have succeeded in crystallizing two types of new salts, **4** and **5**. The effective magnetic moment observed for **4** ($\mu_{eff} = 2.06\mu_B$, 5−120 K) reflects the $S = {}^1/_2$ character responsible for Pt(2.25+)$_4$, as previously observed for some Pt(2.25+)$_4$ analogues ($\mu_{eff} = (1.81-1.94)\mu_B$).[6c,h] The structure of **4** is shown in Figure 3 (a view for **5** in Figure S1). No axial donor is bound to the terminal Pt atoms. As

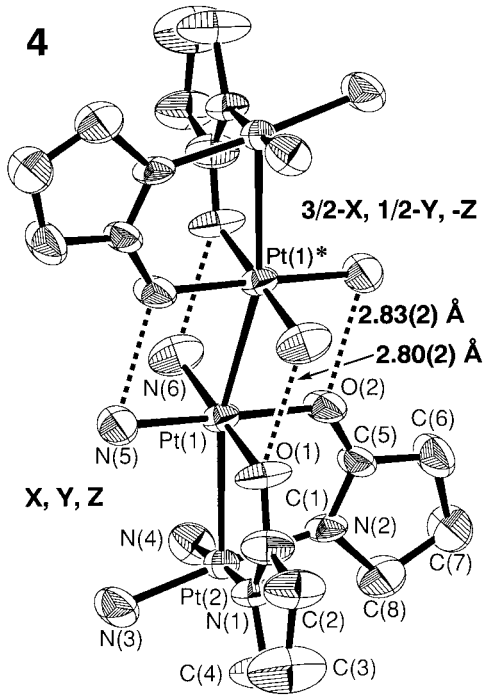

Figure 3. ORTEP drawing of HH-$[Pt(2.25+)_2(NH_3)_4(\mu\text{-}C_4H_6NO)_2]_2^{5+}$ in **4** (50% thermal ellipsoids), where dotted lines denote hydrogen bonds. Selected interatomic distances (Å) and angles (deg): Pt(1)−Pt(2) = 2.8780(9); Pt(1)−Pt(1)* = 2.894(1); Pt(1)*−Pt(1)−Pt(2) = 165.57(4); Pt(1)−O(1) = 2.017(9); Pt(1)−O(2) = 2.02(1); Pt(1)−N(5) = 2.03(1); Pt(1)−N(6) = 2.02(1); Pt(2)−N(1) = 2.02(1); Pt(2)−N(2) = 1.99(1); Pt(2)−N(3) = 2.03(1); Pt(2)−N(4) = 2.05(1); O(1)−C(1) = 1.27(2); O(2)−C(5) = 1.28(1); N(1)−C(1) = 1.27(2); N(2)−C(5) = 1.31(2); Pt(1)−O(1)−C(1) = 121.1(10); Pt(1)−O(2)−C(5) = 121.9(10); Pt(2)−N(1)−C(1) = 126(1); Pt(2)−N(2)−C(5) = 129(1); O(1)−C(1)−N(1) = 128(1); O(2)−C(5)−N(2) = 125(1).

summarized in Table 3, **4** and **5** possess very similar structural features, implying that their structures are little affected by the difference in the packing environment. Importantly, the intradimer Pt−Pt distances of **4** and **5** are ca. 0.1 Å longer than those of the α-pyridonate and 1-methyluracilate blues (**16** and **20**). On the other hand, the interdimer Pt−Pt distances are comparable to those in **16** and **20**.

Stoichiometric Green and Cl-Coordinated Pt(2.5+)$_4$. During the above efforts, we encountered the second green salt **7**. As observed for the first one (**6**), crystals of **7** similarly possess both green-colored and red-colored faces. Although **6** was previously judged to be a nonstoichiometric mixture of Pt(2.25+)$_4$ and Pt(2.5+)$_4$ based on the effective magnetic moment,[8e] **7** has turned out to be a clear 1:1 mixture of them (see Figure 4).

The $S = {}^1/_2$ character over the formula unit was roughly ascertained by the magnetic susceptibility measurement carried out for a very small quantity of **7** ($\mu_{eff} = 1.79\mu_B$, 5−12 K). The Pt(2.25+)$_4$ cation (**7a**) has almost the same structure as **4** and **5** (see Table 3 and a view for **7a** in Figure S2), which again suggests that the structure of Pt(2.25+)$_4$ is little affected by the packing environment. More interestingly, the Pt(2.5+)$_4$ cation (**7b**) is axially ligated with two oxygen atoms of nitrates at both ends of the unit (Pt−O(nitrate) = 2.52(2) Å, a view for **7b** in Figure S3). Although two nitrate ions in **8** are loosely bound to the terminal Pt atoms (Pt···O(nitrate) = 2.715(10) and 2.603(10) Å),[8g] the distances are too long to suggest the axial ligation ability of Pt(2.5+)$_4$. The here observed distance (2.52(2) Å) is still long for a normal single bond between Pt and O but is not amazingly long in comparison with the Pt−O(axial nitrate)

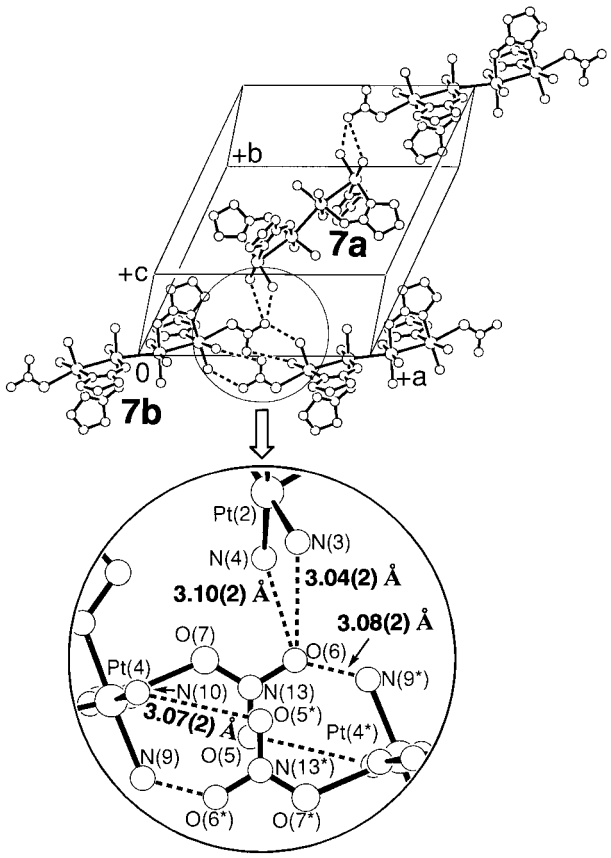

Figure 4. Crystal packing arrangement of HH-$[Pt(2.5+)_2(NH_3)_4(\mu\text{-}C_4H_6NO)_2(NO_3)]_2^{4+}$ (at (0 0 0)) and HH-$[Pt(2.25+)_2(NH_3)_4(\mu\text{-}C_4H_6NO)_2]_2^{5+}$ (at (1/2 1/2 1/2)) in **7** (top). For clarity, atoms are drawn with ideal spheres, and counterions and water molecules are omitted. Hydrogen bonds are drawn with dotted lines. The magnification (bottom) shows intercationic hydrogen bonding and π-stacking, viewed perpendicular to the stacked NO_3^- planes, where O(5)···O(5*) = 2.98(3), O(5)···N(13*) = 3.04(2), Pt(2)···Pt(4) = 6.380(1), Pt(2)···Pt(4*) = 7.684(1), and Pt(4)···Pt(4*) = 7.290(1) Å.

Scheme 1

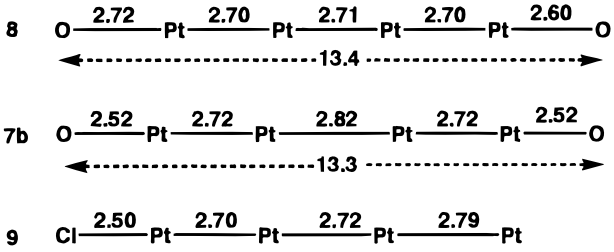

distances previously observed for the α-pyrrolidinonate Pt(3.0+)$_2$ (2.29(1)−2.36(2) Å).[8h−j] We think the present result is a more convincing one to suggest that Pt(2.5+)$_4$ takes axial donors *even in solution*. Further, the difference in the Pt−O(nitrate) distance between **7b** and **8** can be reasonably explained in terms of Scheme 1. The axial coordination distances in **7b** are shortened, but the central Pt−Pt bond length in **7b** is elongated, while the change in the bridged Pt−Pt distance is trivial. In addition, the sum of five bond lengths over the O−Pt$_4$−O chain is unchanged. A qualitative aspect is that the bonding character at the central Pt−Pt bond is partially shifted to the terminal Pt−O bonds in going from **8** to **7b**.

In addition to the above results, we have also succeeded in isolating the second example, **9**, demonstrating the axial ligation ability of Pt(2.5+)$_4$. As shown in Figure 5, the Pt(2.5+)$_4$ unit in **9** is singly coordinated by a chloride ion, and it therefore

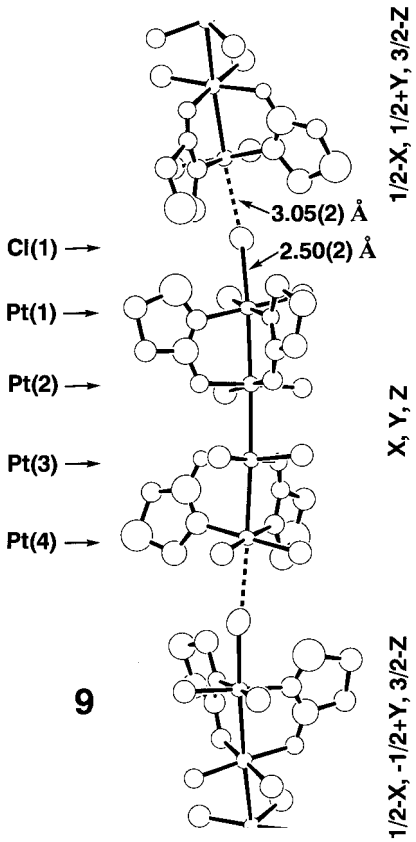

Figure 5. Pseudo-1D network, HH-$[Pt(2.5+)_4(NH_3)_8(\mu\text{-}C_4H_6NO)_4(Cl)]_n^{5n+}$, in **9** (50% thermal ellipsoids). Selected interatomic distances (Å) and angles (deg): Pt(1)−Pt(2) = 2.701(4); Pt(2)−Pt(3) = 2.724(4); Pt(3)−Pt(4) = 2.793(4); Pt(1)−Pt(2)−Pt(3) = 171.6(1); Pt(2)−Pt(3)−Pt(4) = 168.3(1); Pt(2)−Pt(1)−Cl(1) = 173.8(4); Pt(1)−Cl(1)−Pt(4)* = 168.8(7); Cl(1)−Pt(4)*−Pt(3)* = 176.1(4).

possesses a vacant axial coordination site as well. The Pt−Cl distance of 2.50(2) Å in **9** is rather close to the values of Pt−Cl = 2.361(4)−2.455(4) Å observed for the monochloro- and dichloro-coordinated α-pyrrolidinonate $Pt(3.0+)_2$ (**11** and **12**; vide infra). Moreover, the axial bond order in **9** must be much higher than those of **7b**, because the axial bond lengths of **9** and **7b** are similar despite that the bonding radius of Cl is 0.2−0.3 Å longer than that of O. As illustrated in Scheme 1, it can be qualitatively considered that the bonding nature over the two axial bonds in **7b** is now condensed into the single axial bond in **9**. There is no difference in the sum of three Pt−Pt bond lengths between **7b** and **9**. However, an asymmetric character is strongly enhanced in **9** (see Scheme 1), indicating that the Pt−Pt bonding nature is more localized over the Cl-coordinated unit. In other words, the two inner Pt atoms in **8** must have a higher net oxidation state than those in **7b**. In **9**, the Pt atoms within the Cl-coordinated unit have a higher net oxidation state than those in the other unit. Thus, the delocalization pattern strongly depends on what donors are bound to the axial coordination sites.

On the other hand, the terminal Cl ion in **9** has a weak interaction with the vacant axial coordination site in the adjacent tetramer, giving a very attractive pseudo-1D framework with an expression of $[Pt(2.5+)_4-Cl\cdots]_\infty$ (see Figure 5). This can be viewed as related to the $[Pt(II)\cdots Cl-Pt(IV)\text{-}Cl\cdots]_\infty$ framework of the Wolffram's red salt, $[Pt(II)(NH_2Et)_4][Pt(IV)(NH_2Et)_4Cl_2]Cl_4\cdot 4H_2O$.[30] This type of linear halide-bridged systems has been extensively studied in recent years for the fabrication of new conducting materials.[30,31] In addition, quadruply bridged dimers, $[Pt_2(\mu\text{-dithioacetato})_4-X]$[32] and $[Pt_2(\mu\text{-pop})_4-X]$[33] (pop = $P_2O_5H_2$), are known to give analogous chains $[X-Pt(3.0+)_2-X\cdots Pt(2.0+)_2\cdots]_\infty$ (or $[Pt(2.5+)_2-X]_\infty$), and attractive metallic conduction was very recently reported on the dithioacetate system.[32c] The Pt···Cl distance in **9** (3.05(2) Å) is comparable to those previously reported for the $[PtCl]_\infty$ and $[PtPtCl]_\infty$ systems (e.g., 3.13 Å for $[Pt(II)(NH_2Et)_4][Pt(IV)(NH_2Et)_4Cl_2]Cl_4\cdot 4H_2O$[30,34] and 3.022(4) Å for $(NH_4)_4[Pt_2(\mu\text{-pop})_4Cl]$[33b]). The inter-tetramer Pt···Pt distance is only slightly shorter than the sum of the Pt−Cl and Cl···Pt distances (5.521(4) Å), reflecting the linearity of the chain (see also Figure 5). Thus, the present system can be regarded as the third type of quasi-1D halide-bridged system and must be distinguished from the previous systems because of the higher mobility of electrons within the repeating unit. Further studies on this system are now in progress.

Monochloro- and Dichloro-Coordinated $Pt(3.0+)_2$. We briefly reported on the following equilibria ($K_1 = 1.7 \times 10^5$ and $K_2 = 4.0 \times 10^3$ M^{-1}).[35]

$$H_2O-Pt(3.0+)_2-OH_2 + Cl^- \rightleftharpoons H_2O-Pt(3.0+)_2-Cl \quad (3)$$

$$H_2O-Pt(3.0+)_2-Cl + Cl^- \rightleftharpoons Cl-Pt(3.0+)_2-Cl \quad (4)$$

In the spectrophotometric titration experiments, a clear isosbestic point was observed when the equilibrium shift in eq 3 was predominant. This fact suggests that the first ligation of Cl^- selectively occurs at one of the two chemically nonequivalent Pt atoms in the *head-to-head* dimer (N_2O_2- and N_4-coordinated Pt atoms), for two possible monochloro species are likely to possess slightly different spectral features. The same behavior was also observed for the substitution reaction with SO_4^{2-}.[13] To further clarify these behaviors, we attempted to isolate the monochloro species **12**. During this effort, we also isolated the dichloro complex **11**. Their crystal structures are shown in Figure 6. **12** is the first example of the monochloro species. The structure indirectly suggests that the N_2O_2-Pt atom has higher acceptor ability than the N_4-Pt one. This must be related to the higher electronegativity of oxygen atoms, leading to a higher net charge at the N_2O_2-Pt atom. Such evidence was also provided by the structure analysis of a 1-methyluracilate-bridged $HH-Pt(3.0+)_2-NO_2$ dimer which possesses no axial

(30) (a) Keller, H. J. *Extended Linear Chain Compounds*; Miller, J. S., Ed.; Plenum Press: New York, 1982; Vol. 1, p 357. (b) Keller, H. J., Ed. *Chemistry and Physics of One Dimensional Metals*; Plenum Press: New York, 1977. (c) Day, P. *Low Dimensional Cooperative Phenomena*; Keller, H. J., Ed.; Plenum Press: New York, 1974; p 191.

(31) (a) Clark, R. J. H.; Michael D. J.; Yamashita, M. *J. Chem. Soc., Dalton Trans.* **1991**, 725. (b) Iwasa, Y.; Funatsu, E.; Koda, T.; Yamashita, M.; Kobayashi, H.; Kubodera, K. *Mol. Cryst. Liq. Cryst. Sci. Technol.* **1992**, *217*, 37. (c) Okamoto, H.; Mitani, T.; Toriumi, K.; Yamashita, M. *Phys. Rev. Lett.* **1992**, *69*, 2248. (d) Toriumi, K.; Yamashita, M.; Kurita, S.; Murase, I.; Ito, T. *Acta Crystallogr.* **1993**, *B49*, 497. (e) Okamoto, H.; Mitani, T.; Toriumi, K.; Yamashita, M. *Mater. Sci. Eng.* **1992**, *B13*, L9. (f) Okamoto, H.; Shimada, Y.; Oka, Y.; Chainani, A.; Takahashi, T.; Kitagawa, H.; Mitani, T.; Toriumi, K.; Inoue, K.; Manabe, T.; Yamashita, M. *Phys. Rev. B* **1996**, *54*, 8438. (g) Okamoto, H.; Oka, Y.; Mitani, T.; Yamashita, M. *Phys. Rev. B* **1997**, *55*, 6330.

(32) (a) Bellitto, C.; Flamini, A.; Gastaldi, L.; Scaramuzza, L. *Inorg. Chem.* **1983**, *22*, 444. (b) Yamashita, M.; Wada, Y.; Toriumi, K.; Mitani, T. *Mol. Cryst. Liq. Cryst. Sci. Technol.* **1992**, *216*, 207. (c) Kitagawa, H.; Onodera, N.; Ahn, J. S.; Mitani, T.; Toriumi, K.; Yamashita, M. *Synth. Met.* **1997**, *86*, 1931.

(33) (a) Buttler, L. G.; Zietlow, M. H.; Che, C. M.; Schaefer, W. P.; Sridhar, S.; Grunthaner, P. J.; Swanson, B. I.; Clark, R. J. H.; Gray, H. B. *J. Am. Chem. Soc.* **1988**, *110*, 1155. (b) Jin, S.; Ito, T.; Toriumi, K.; Yamashita, M. *Acta Crystallogr.* **1989**, *C45*, 1415. (c) Yamashita, M.; Toriumi, K. *Inorg. Chim. Acta* **1990**, *178*, 143.

(34) Craven, B. M.; Hall, D. *Acta Crystallogr.* **1961**, *14*, 475.

(35) Sakai, K.; Tsuchiya, Y.; Tsubomura, T. *Technol. Rep. Seikei University* **1992**, *54*, 77−78 (private communication).

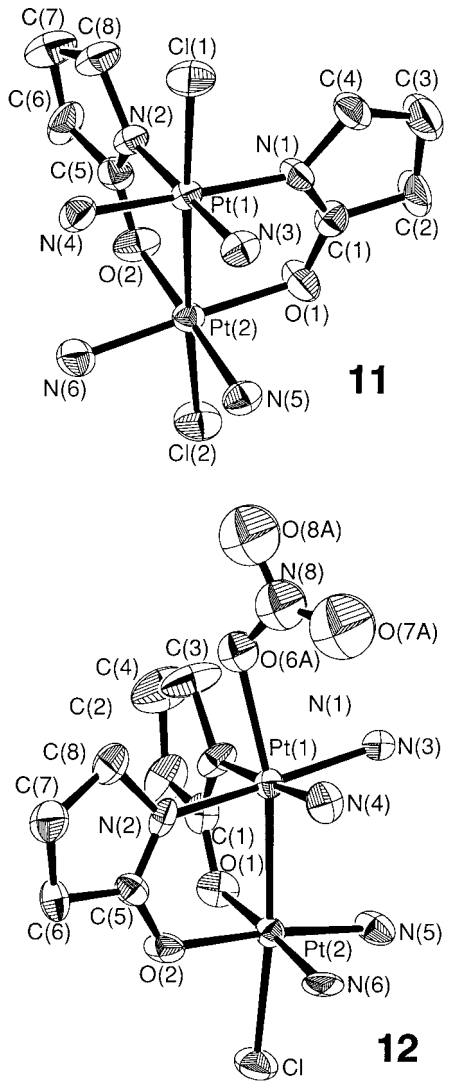

Figure 6. ORTEP views (50% thermal ellipsoids) for HH-$[Pt(3.0+)_2(NH_3)_4(\mu\text{-}C_4H_6NO)_2(Cl)_2]^{2+}$ in **11** (top) and HH-$[Pt(3.0+)_2(NH_3)_4(\mu\text{-}C_4H_6NO)_2(Cl)(NO_3)]^{2+}$ in **12** (bottom). For the latter, only one of the two disordered nitrate ions (A) is shown for clarity.

donor at the N_4−Pt atom.[3b] However, we still cannot abandon a possibility that the other type of monochloro-coordinated species (N_4−Pt−Cl species) is present as a minor species in solution.

The axial Pt−Cl distances in the dichloro complex **11** (2.395(3) and 2.455(4) Å) are comparable to those for the two reported analogues (2.425(4) and 2.459(3) Å for the 1-methyluracilate HH−$Pt(3.0+)_2$[3c] and 2.429(2) and 2.444(2) Å for the α-pyridonate HH−$Pt(3.0+)_2$[7c]). On the other hand, the Pt−Cl distance in the monochloro complex **12** (2.361(4) Å) is effectively shorter than those discussed above but is still longer than those for the common platinum complexes, such as $PtCl_4^{2-}$ (2.30 Å),[36] *cis*-$Pt(NH_3)_2Cl_2$ (2.31 Å),[37] and $PtCl_6^{2-}$ (2.30−2.32 Å).[36] The Pt−O(nitrate) distance in **12** is 2.29 Å (2.30(3) Å for A and 2.27(3) Å for B).

On the other hand, **11** and **12** both display a color change to red or blue upon exposure to air for several months in the solid state. These behaviors have a close resemblance to the color-change phenomenon exhibited by the *purported* tetraplatinum-

(36) Bisi-Castellani, C.; Lanfredi, A. M. M.; Tiripicchio, A.; Maresca, L.; Natile, G. *Inorg. Chim. Acta* **1984**, *90*, 155.

(37) Raudaschl, G.; Lippert, B.; Hoeshele, J. D.; Howard-Lock, H. E.; Lock, C. J. L.; Pilon, P. *Inorg. Chim. Acta* **1985**, *106*, 141.

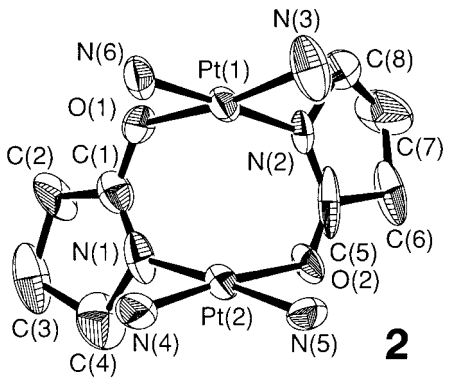

Figure 7. ORTEP drawing for HT-$[Pt(2.0+)_2(NH_3)_4(\mu\text{-}C_4H_6NO)_2]^{2+}$ in **2** (50% thermal ellipsoids). The shortest interdimer Pt−Pt distance is 5.8515(7) Å.

(III) complex, $[Pt(3.0+)_2(NH_3)_4(\mu\text{-}\alpha\text{-pyrrolidinonato-}N,O)_2]_2^{8+}$ (**23**).[8k] It was reported that **23** is fairly labile in air at room temperature and shows a color change to red and then to blue in the solid state, where formation of $Pt(2.25+)_4$ was only *qualitatively* confirmed by EPR. However, the above observations clearly point out that such solid-state properties should not be regarded as evidence of a tetranuclear structure in the starting solid. The rate of color change strongly depends on the kinds of axial donors, and stability becomes lower in the order of O_2NO−$Pt(3.0+)_2$−NO_2 (**10**) ∼ Cl−$Pt(3.0+)_2$−Cl (**11**) > O_2NO−$Pt(3.0+)_2$−Cl (**12**) ≫ **23** (presumably, H_2O−$Pt(3.0+)_2$−OSO_4, etc.). We now believe that the highly air-sensitive nature of **23** must be responsible for the lability of the axial bonds, for the total stability constant for the sulfato-coordinated species is much smaller than those for the chloro- and nitro-coordinated ones.[13,15,35]

HT-Pt(2.0+)$_2$. An ORTEP drawing for the α-pyrrolidinonate HT dimer **2** is shown in Figure 7. The bridged Pt−Pt distance (3.085(1) Å) is effectively longer than the value of 3.029(2) Å reported for the α-pyrrolidinonate HH analogue (**1**).[8b] The same tendency has been observed in other ligand systems (e.g., 2.8767(7) (HH)[5a,b] and 2.8981(5) (HT)[5a,b] Å for α-pyridonate; 2.937(1) (HH)[3e] and 2.954(2) (HT)[3a] Å for 1-methyluracilate; 2.927(1) (HH)[4a,b] and 2.974(1) (HT)[4c] Å for 1-methylthyminate). Therefore, it can be generally considered that the bridged Pt−Pt distance of HT-$Pt(2.0+)_2$ is longer than that of HH−$Pt(2.0+)_2$ in each ligand system. It is also noteworthy that this is the first HT dimer for which spontaneous resolution is observed (space group $P2_1$), for all the previously reported HT dimers crystallize in a centrosymmetric space group.[3a,4c,5b,10a]

OH-Bridged Dimer of HT-Pt(3.0+)$_2$. The tetranuclear cation in **14** has a structure very similar to that in **13** (Figure 8). However, **14** is different from **13** in three ways, that is, (i) the terminal ligands, (ii) the bridging arrangement of amidates, and (iii) the central bridging units are different from each other (see Table 1). In **14**, the dimer−dimer association is also stabilized by two hydrogen bonds formed between the ammines and the oxygen atoms of the α-pyrrolidinonates. A hydrogen bond is also formed between the ammine and the oxygen atom of μ-OH within the dimer unit, which can be correlated with the exceptionally short bridged Pt−Pt distance (2.5527(7) Å; see Table 3).

Structural Transformation of U-Shaped Dimeric Units upon Changing Pt Oxidation States. It has been assumed that the Pt−Pt distances are predominantly controlled by the Pt−Pt bond order based on the average Pt oxidation state (abbreviated as Pt-ox) and are not significantly affected by the individual structural features of amidates.[5b,7b,d,8c−g] However,

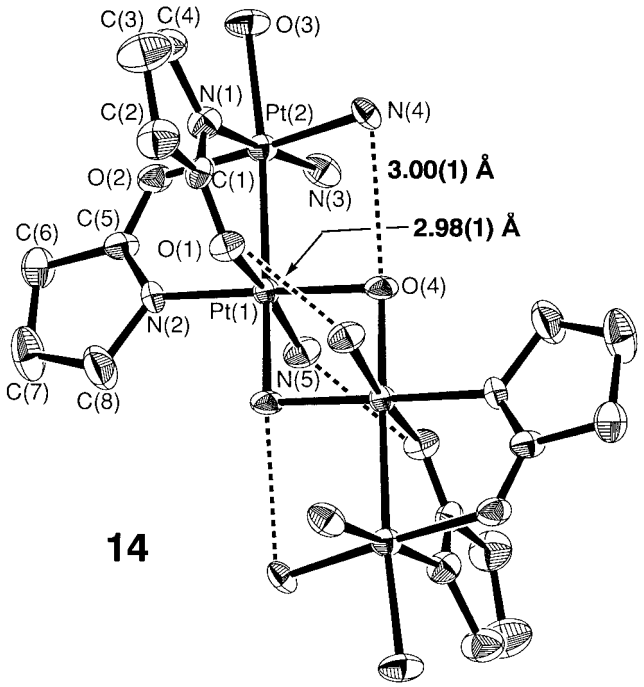

Figure 8. ORTEP drawing for HT-$[(H_2O)(H_3N)_2Pt(3.0+)(\mu\text{-}C_4H_6NO)_2Pt(3.0+)(NH_3)(\mu\text{-}OH)]_2^{6+}$ in **14** (50% thermal ellipsoids), where dotted lines denote hydrogen bonds. Selected interatomic distances (Å) and angles (deg): Pt(1)−Pt(2) = 2.5527(7); Pt(1)−Pt(1)^a = 3.1578(6); Pt(1)−O(1) = 2.015(6); Pt(1)−O(4) = 2.035(5); Pt(1)−O(4)^a = 2.112(6); Pt(1)−N(2) = 1.986(6); Pt(1)−N(5) = 2.013(7); Pt(2)−O(2) = 2.037(6); Pt(2)−O(3) = 2.188(6); Pt(2)−N(1) = 2.008(7); Pt(2)−N(3) = 2.068(7); Pt(2)−N(4) = 2.027(6); Pt(1)−O(4)−Pt(1)^a = 99.2(2); O(1)−Pt(1)−O(4) = 88.2(2); O(1)−Pt(1)−O(4)^a = 84.6(2); O(1)−Pt(1)−N(2) = 91.1(2); O(1)−Pt(1)−N(5) = 171.7(3); O(4)−Pt(1)−O(4)^a = 80.8(2); O(4)−Pt(1)−N(2) = 178.5(3); O(4)−Pt(1)−N(5) = 92.2(2); O(4)^a−Pt(1)−N(2) = 97.8(3); O(4)^a−Pt(1)−N(5) = 87.2(3); N(2)−Pt(1)−N(5) = 88.3(3); O(2)−Pt(2)−O(3) = 90.2(2); O(2)−Pt(2)−N(1) = 91.0(3); O(2)−Pt(2)−N(3) = 89.6(3); O(2)−Pt(2)−N(4) = 177.4(3); O(3)−Pt(2)−N(1) = 90.8(3); O(3)−Pt(2)−N(3) = 87.7(3); O(3)−Pt(2)−N(4) = 87.9(3); N(1)−Pt(2)−N(3) = 178.4(3); N(1)−Pt(2)−N(4) = 87.2(3); N(3)−Pt(2)−N(4) = 92.2(3), where the symmetry operation for O(4)^a and Pt(1)^a is $1 - X, -Y, -Z$.

Scheme 2

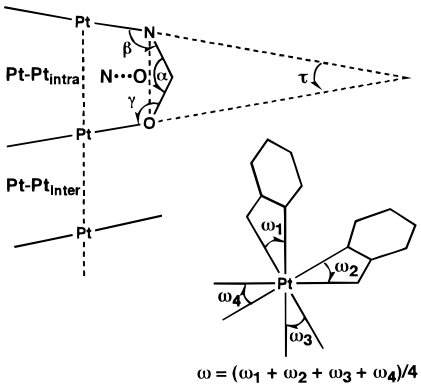

careful inspection now allows us to discuss the latter components. Here we will look into several important structural parameters on the HH units (Scheme 2) as a function of Pt-ox. The definition of τ is also given in Table 3. Since trivial changes in the Pt−O, Pt−N, C−O, and N−C distances do not induce any pronounced change in Pt−Pt$_{intra}$, they will not be discussed.

First of all, it is now clear from Figure 9a that the relationship between Pt−Pt$_{intra}$ and Pt-ox ({Pt−Pt$_{intra}$}−{Pt-ox}) for the

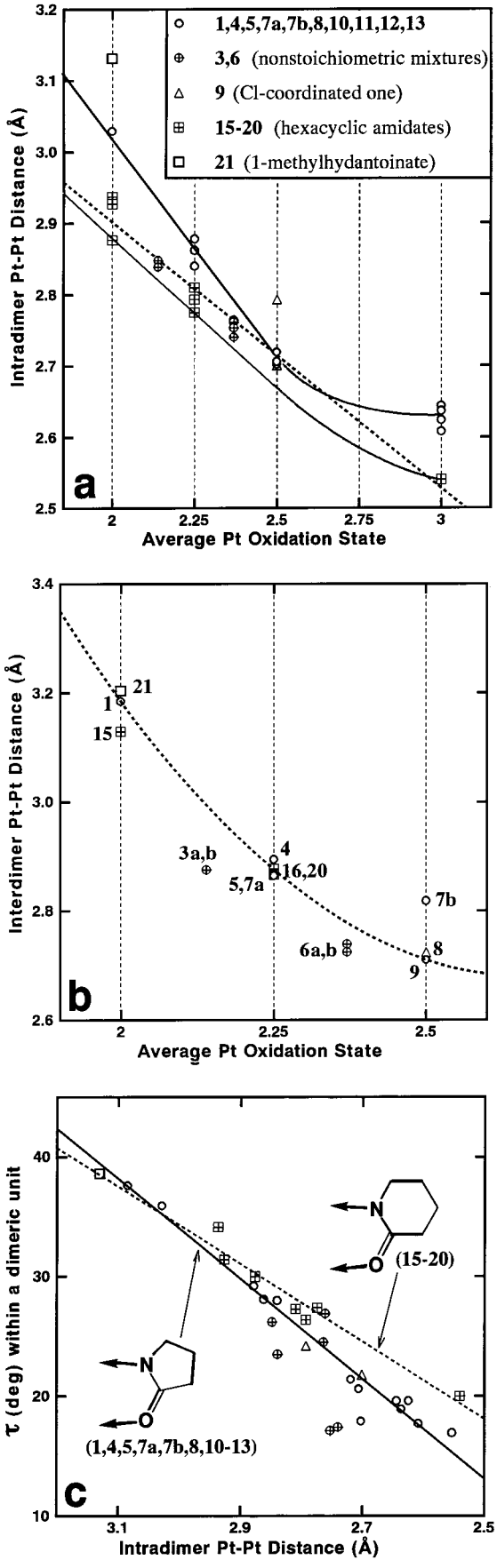

Figure 9. Structural Relationships for (a) {Pt−Pt$_{intra}$}−{Pt-ox}, (b) {Pt−Pt$_{inter}$}−{Pt-ox}, and (c) {τ}−{Pt−Pt$_{intra}$}.

α-pyrrolidinonate system is amazingly different from that for the α-pyridonate system (compare two solid lines). The dotted

Scheme 3

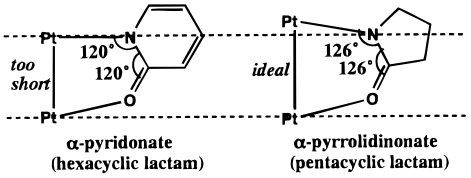

line is defined with the hexacyclic amidate compounds **15**−**20**, satisfies the distance parameter of the α-pyrrolidinonate Pt-(2.5+)$_4$ (**8**), and was used to evaluate those of the *nonstoichiometric mixtures* **3** and **6**.[8c−e] While the structural parameters rather indicate that **3** has an oxidation level of 2.25+ (see also Figure 9b), a straightforward comment cannot be given. However, further discussion is meaningless because of the unreasonably wide distribution of N···O in **3**, **6**, and **8** (see Table 3). The data for the rest of the α-pyrrolidinonate compounds indicate that N···O is essentially unaffected by a change in Pt−Pt$_{intra}$ and is ca. 2.3 Å in any case. Another important feature provided with the {ω}−{Pt-ox} relationship is that ω essentially remains unchanged upon changing Pt−Pt$_{intra}$ (or Pt-ox) in both the α-pyrrolidinonate (0−6°) and α-pyridonate (20−23°) systems (Table 3), although the values are quite different between the two systems. Therefore, it is not reasonable to consider that the "U-shaped dimers afford a twist in ω upon the shortening of Pt−Pt$_{intra}$ so as to avoid the steric contacts between the equatorial ammines". Consequently, we have found that a change in Pt−Pt$_{intra}$ is predominantly compensated for by the τ component (see Figure 9c).

Since τ is mainly determined by α, β, and γ, we further attempted to clarify which component is predominant. Although a clear solution could not be given due to the fairly broad nature in the angle information, careful inspection of α, β, and γ (Table 3) raises the following points: (i) τ is predominantly controlled by Pt−O−C (γ) rather than by P−N−C (β) in the α-pyridonate system (the sp^2-hybridized nature must be responsible for the higher rigidity in β); (ii) τ is controlled by both Pt−O−C (γ) and P−N−C (β) in the α-pyrrolidinonate system; (iii) O−C−N (α) is rather insensitive to τ in both systems; (iv) O−C−N (α) and Pt−N−C (β) in the α-pyrrolidinonate system are both larger by 3−5° than those in the α-pyridonate one. The last point indicates that the marked difference observed between the two systems (Figure 9a) is largely attributable to the fundamental differences in the ideal O−C−N and Pt−N−C angles (see Scheme 3).

As illustrated in Scheme 3, if the two bridged Pt atoms are located on the plane defined with an α-pyridonate ligand (ω = 0°), then Pt−Pt$_{intra}$ will become too short. To afford a longer Pt−Pt distance without causing too much strain about α and β, the two Pt atoms will be shifted out of the plane upward and downward, respectively, resulting in an increase in ω. On the other hand, there should be no necessity for the α-pyrrolidinonate dimer to give a twist in ω owing to the larger ideal angles of α and β. The overall strain energy is expected to be high in the α-pyridonate system, whereas the steric strain must be relatively small in the α-pyrrolidinonate system.

Importantly, the above finding can be viewed as related to the difference between the two systems in the rate of HH−HT isomerization of Pt(2.0+)$_2$, that is, the isomerization is extremely slow in the α-pyridonate system (it takes several months)[5d,e] and quite rapid in the α-pyrrolidinonate one (it takes place immediately after dissolution).[8b] It seems probable that the α-pyrrolidinonate dimer can afford a relatively large extent of distortion leading to the HH−HT conversion, since it is little strained. On the other hand, the α-pyridonate dimer cannot afford such distortion, for the molecule is already strained. It was reported that dissociative activation is responsible for the HH−HT isomerization of [Pt(2.0+)$_2$(en)$_2$(μ-α-pyridonato)$_2$]$^{2+}$.[8d,e] If the above two systems obey the same mechanism, the higher structural flexibility of the α-pyrrolidinonate dimer must facilitate the dissociative activation of the molecule. Additionally, we further assumed that such a structural difference might be correlated to the fact that the hexacyclic amidate Pt(2.5+)$_4$ has never been isolated. However, our study on the α-pyridonate system (see Experimental Section) reveals that this is not the case. Nevertheless, this is an important result as concrete evidence showing the existence of a complex which has only been postulated so far.

Scheme 4

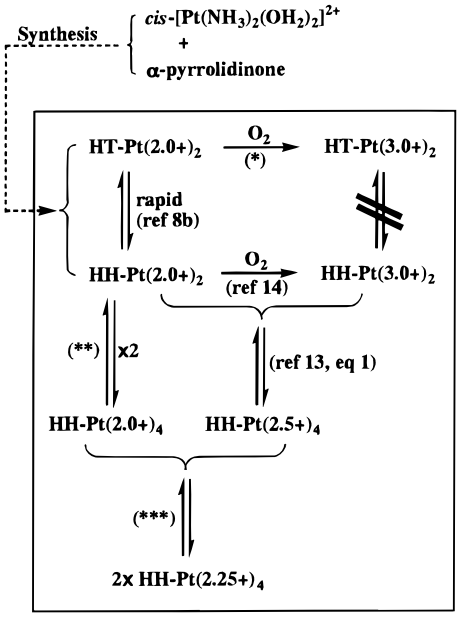

Finally, it is important to note that the rigidity in O−C−N will be lost when acyclic amidates, such as acetamidate, are employed instead of exocyclic amidates. In these cases, the dimer units do not need to generate a large twist in ω upon the shortening of Pt−Pt$_{intra}$ but vary the τ component by changing all three components (α−γ).[11,12,38]

Solution Properties. The solution properties of the platinum-blue complexes can be rationally understood in terms of the previously characterized processes together with several postulated processes (asterisked ones) in Scheme 4. Cyclic voltammograms of the α-pyrrolidinonate compounds display only a quasi-reversible[8a] or reversible[39] Pt-based wave in any condition, indicating that the Pt(2.0+)$_2$/Pt(3.0+)$_2$ couples of HH and HT have similar potentials, as observed in the α-pyridonate system.[7a,b] Therefore, the postulation of "*" appears quite reasonable. The HH−HT isomerization process of Pt(3.0+)$_2$

(38) Several new Pt(2.0+)$_2$ analogues bridged by R−CONH (*N*-methylisonicotinamidate,[21c,d] *N*-methylnicotinamidate,[21d] and *N*-(carbamoylmethyl)pyridinium[21d]) have been structurally characterized, and no considerable twist in ω was observed in each case. The details will be separately reported elsewhere.

(39) Sakai, K.; Tsuchiya, Y.; Tsubomura, T. *63rd Annual Meeting Chem. Soc. Jpn.* **1992**, 3C132 (domestic meeting). The study showed that **11** displays a highly reversible wave (ΔE_p = 32 mV), which is ideal for a 2e$^-$ process, in the presence of Cl$^-$. Moreover, $E_{1/2}$ was observed to be linear to −ln [Cl$^-$] with a slope consistent with the equation [Pt(2.0+)$_2$]$^{2+}$ + 2Cl$^-$ ⇌ [Cl−Pt(3.0+)$_2$−Cl]$^{2+}$ + 2e$^-$. In addition, quite identical waves were observed when **8** was employed instead of **11**, in agreement with the fact that eq 1 is largely shifted to the side of dimers.[13] The details will be separately reported elsewhere.

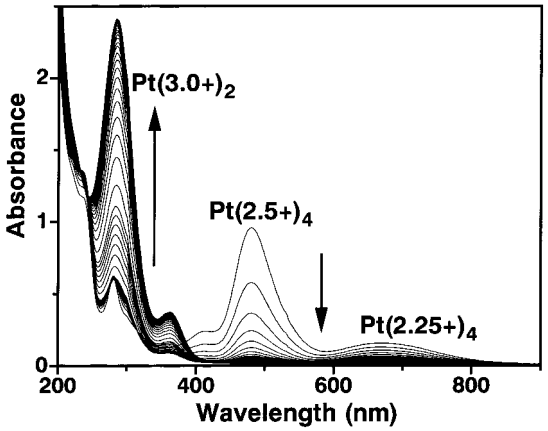

Figure 10. Time-course changes of UV−vis absorption spectra after dissolution of **4** into 1.00 M H_2SO_4 (7.53×10^{-5} M) at 25 °C in air. Scanning time: first 15 scans, 34−874 s, every 1 min; second 7 scans, 1774−7162 s, every 15 min; third 30 scans, 9572−113970 s, every 1 h (not all the data recorded are shown).

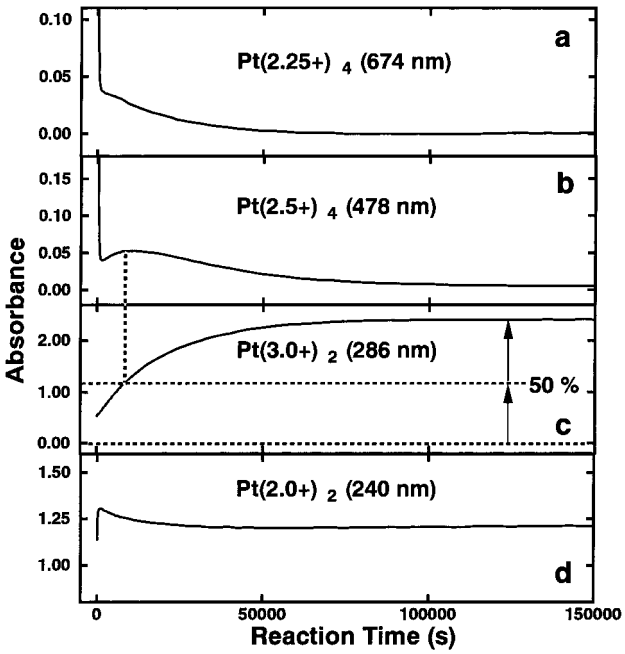

Figure 11. Absorbance-change profiles for the experiment in Figure 10.

can be excluded, as it has never been observed to date (Pt(3.0+)$_2$ must be rigid due to the single bond between the metals). "**" and "***" might arouse some controversies, for it has been a common belief that Pt(2.0+)$_4$ completely cleaves into dimers in solution and some assumed that the oxidation processes of this family occur *in a stepwise manner*: Pt(2.0+)$_2$ → Pt(2.25+)$_4$ → Pt(2.5+)$_4$ → Pt(3.0+)$_2$.[3f,8i] However, one must realize now that it is not necessary to consider the stepwise processes to account for the formation of the mixed-valence species. Additionally, it is not necessary to consider the presence of Pt(2.5+)$_2$, which was previously postulated as a precursor for Pt(2.25+)$_4$ (Pt(2.0+)$_2$ + Pt(2.5+)$_2$ ⇌ Pt(2.25+)$_4$).[7a,b,8a,b] The electrochemical behaviors mentioned above also indicate that [Pt(2.5+)$_2$] must be extremely low, if any exists. On the other hand, the reaction rates for the HH−HT isomerization[8b] and the equilibrium shifts in eq 1[13] are much faster than that for the O_2-oxidation of Pt(2.0+)$_2$.[14] If the equilibrium shifts in "**" and "***" are similarly fast, changes in [Pt(2.0+)$_2$] and [Pt(3.0+)$_2$] caused by the O_2-oxidation processes will be rapidly balanced with the overall equilibrium shifts in Scheme 4. Even if the O_2-oxidation processes involve the above stepwise processes, the relative abundances of all the chemical species will be rapidly balanced in the same manner.

An important observation supporting the above concepts is that, when **4** (Pt(2.25+)$_4$) is dissolved into an aqueous H_2SO_4 solution in air, the absorption band at 478 nm corresponding to Pt(2.5+)$_4$[13] is already seen immediately after dissolution of the complex (Figure 10; see also Experimental Section). This suggests that the upward shift in "***" takes place quite rapidly within the dissolution stage. The unobservably rapid character well reflects that this is a simple outer-sphere electron-transfer process. From the initial first-order decay at 478 nm (k_{obs} = 0.0085(1) s^{-1}), [Pt(2.5+)$_4$]$_0$ = 3.76×10^{-5} M ([ ]$_0$ denotes the concentration right at the dissolution time) can be estimated from Abs$_0$(478) = 1.28 and ϵ_{478}(Pt(2.5+)$_4$) = 3.4×10^4 $M^{-1}cm^{-1}$ (see Experimental Section). Therefore, if "**" and "***" are the only reactions that take place within the dissolution stage and if [Pt(2.0+)$_4$] is negligibly small, [Pt(2.0+)$_2$]$_0$ = 7.52×10^{-5} M can be deduced. These values together with a value of [Pt(2.25+)$_4$]$_{dissolved}$ = 7.53×10^{-5} M, calibrated from the final absorbance at 362 nm, afford an estimate that [Pt(2.25+)$_4$]$_0$ is extremely low, suggesting that "***" rapidly ends within the dissolution stage and that ϵ_{674}(Pt(2.25+)$_4$) is much larger than ϵ_{478}(Pt(2.5+)$_4$). Although ϵ_{674}(Pt(2.25+)$_4$) still remains undetermined, our tentative prediction of ϵ_{674}(Pt(2.25+)$_4$) > 10^5 M^{-1} cm^{-1} is consistent with the results obtained by the simultaneous measurements of absorbance at 674 nm and the spin density (S = $^1/_2$ for Pt(2.25+)$_4$). Another source of support for "**" and "***" is that, when the same experiment was performed by dissolving Pt(2.5+)$_4$ (**8**), the band at 674 nm initially increases and then decreases as the disproportionation reaction (eq 1) proceeds.[40] This suggests that Pt(2.0+)$_2$ formed by eq 1 is required for the formation of Pt(2.25+)$_4$. On the other hand, the bands at 240−400 nm, which correspond to the mono- and disulfato Pt(3.0+)$_2$ species,[13] gradually increase over a day. Absorbance changes at 286 nm (Figure 11c) obey a first-order process, and the observed rate constant (k_{obs} = 4.85(3) $\times 10^{-5}$ s^{-1}) is in good agreement with those previously observed for the air-oxidation of Pt(2.0+)$_2$ into Pt(3.0+)$_2$ (4.2×10^{-5} s^{-1}, 0.20−0.51 M H_2SO_4, air, 25 °C),[14] implying that the stepwise processes are indeed negligible. Although the absorptivity of Pt(2.0+)$_2$ at wavelengths above 260 nm is negligibly small,[13,18b] the decrease in [Pt(2.0+)$_2$] can be monitored at 240 nm (see Figure 11d). It is important to note here that the absorption bands of Pt(3.0+)$_2$ completely satisfy Beer's law (see Experimental Section), excluding the presence of "Pt(3.0+)$_4$".

A preliminary global kinetic analysis of the spectral changes in Figure 10, together with those on several additional runs carried out by dissolving either **4** or **8**, has been performed to obtain a clear solution for the kinetic profiles using the SPECFIT program.[41] The SVD (factor) analysis of the data sets revealed the presence of four colored components during the course of the reaction, indicating that [Pt(2.0+)$_4$] is indeed negligibly small. So, we attempted to fit the spectral changes to a simplified model that neglects the presence of Pt(2.0+)$_4$ (C → D, C + D ⇌ B, and B + 2C ⇌ 2A; A−D correspond to Pt(2.25+)$_4$, Pt(2.5+)$_4$, Pt(2.0+)$_2$, and Pt(3.0+)$_2$, respectively), where the HH and HT isomers for both Pt(2.0+)$_2$ and Pt(3.0+)$_2$ were assumed to have the same spectral features. The data analysis in SPECFIT was consistent with the overall reaction sequence in this simplified model and returned somewhat

(40) Sakai, K.; Matsumoto, K. *39th Symp. Coord. Chem. Jpn.* **1989**, 1C12 (domestic meeting). Unpublished results.

(41) *SPECFIT*; Spectrum Software Associates: Chapel Hill, NC.

reasonable spectra for species A−D. However, there were some problems in obtaining a reliable predicted spectrum of Pt(2.25+)$_4$. In part, this arises from our lack of knowledge about the equilibrium constant for the first step (overall equilibrium constant for "**" and "***") and from the long scanning time (33 s), which distorts the spectral features during the initial rapid portion of the reaction.

During the slow reaction stage, the absorption band at 478 nm once shows recovery as the UV band increases (Figure 11b). Importantly, the time-course profile in Figure 11b shows a maximum exactly when 50% of the Pt(3.0+)$_2$ is formed (9600 s, as indicated with dotted lines). This is quite consistent with our opinion that [Pt(2.5+)$_4$] is predominantly controlled by eq 1, since Pt(2.0+)$_2$ and Pt(3.0+)$_2$ comprise ca. 98% abundance at this reaction time (the relative abundances of Pt(2.5+)$_4$ and Pt(2.25+)$_4$ are estimated to be 1.2 and <1%, respectively). Furthermore, Figure 11a also reveals that the overall [Pt(II)]/[Pt(III)] ratio must be ca. 3 in order to maximize [Pt(2.25+)$_4$] (neglect the steep region corresponding to the initial rapid process). As a result, it can be considered that (i) the air-oxidation process is predominantly caused by Pt(2.0+)$_2$ → Pt(3.0+)$_2$, (ii) the homovalence dimers are present whenever the mixed-valence tetramers are present (and vice versa), and (iii) the concentrations of the mixed-valence tetramers are varied merely because the overall [Pt(II)]/[Pt(III)] ratio is varied. It should be also noted that these concepts are very important for the platinum-blue syntheses (see Experimental Section).

As for the reaction pathway giving **14**, the formation of HT-Pt(2.0+)$_2$ will be possible right after dissolution of Pt(2.5+)$_4$, according to Scheme 4. However, the overall [HH]/[HT] ratio will be fixed once all the dimeric units are completely oxidized into Pt(3.0+)$_2$ by $S_2O_8^{2-}$. The major Pt(3.0+)$_2$ species under the neutral pH, where the synthesis of **14** was conducted, must be a monohydrolyzed species, $H_2O-Pt(3.0+)_2-OH$ (eq 2).[14,3d] One speculation is that a ligand substitution reaction of an equatorial ammine by the axial hydroxide ion occurs to give a dimer corresponding to a half unit of **14** followed by a rapid axial ligation by an aqua ligand to afford HT-[$(H_2O)(H_3N)_2$Pt(3.0+)(μ-$C_4H_6NO)_2$Pt(3.0+)$(NH_3)(OH)(OH_2)]^{3+}$, which can be dimerized into **14**.

Concluding Remarks. The present studies have provided various important new insights into the chemistry of this family. Although Scheme 4 still does not cover the whole phenomenon that actually takes place in solution, it is now obvious that the axial events for Pt(2.5+)$_4$ must be further clarified in detail. It also seems probable that Pt(2.25+)$_4$ is axially coordinated by water molecules or anions in solution. The detailed equilibrium and kinetic investigations as well as the application research on this family are still in progress in our laboratory.

Acknowledgment. K.S. expresses his deep appreciation to Professor Kazuko Matsumoto (Waseda University), since this study would never have been possible without the knowledge and experimental skill that K.S. acquired while he was a student at her laboratory until 1991. The authors thank Dr. Robert A. Binstead (Spectrum Software Associates) for his kind assistance and helpful discussions on global kinetic analysis with SPECFIT. This work was partly supported by Grants-in-Aid for Scientific Research (Nos. 04854061, 05854065, 06854041, and 07854043) from the Ministry of Education, Science, and Culture of Japan.

Supporting Information Available: Figures S1−S4 showing atom labeling schemes of **5**, **7a**,**b**, and **9** and Tables S1−S32 listing crystallographic details, atomic coordinates, anisotropic thermal parameters, and interatomic distances and angles (53 pages, print/PDF). See any current masthead page for ordering information and Web access instructions.

JA980019Q